FLEXIBLE PRINTED ELECTRONICS FOR TOUCH AND STRAIN FEEDBACK

A THESIS SUBMITTED TO
THE GRADUATE SCHOOL OF ENGINEERING AND SCIENCE
OF BILKENT UNIVERSITY
IN PARTIAL FULFILLMENT OF THE REQUIREMENTS FOR
THE DEGREE OF
MASTER OF SCIENCE
IN
MATERIALS SCIENCE AND NANOTECHNOLOGY

By
Hussain Kawsar Chowdhury
August 2024

Flexible Printed Electronics for Touch and Strain Feedback
By Hussain Kawsar Chowdhury
August 2024

We certify that we have read this thesis and that in our opinion it is fully adequate, in scope and in quality, as a thesis for the degree of Master of Science.

Fatih İnci(Advisor)

Aykut Erbaş

Fatma Yılmaz

Approved for the Graduate School of Engineering and Science:

Orhan Arıkan
Director of the Graduate School

ABSTRACT

FLEXIBLE PRINTED ELECTRONICS FOR TOUCH AND STRAIN FEEDBACK

Hussain Kawsar Chowdhury
M.S. in Materials Science and Nanotechnology
Advisor: Fatih İnci
August 2024

This era of technological revolution demands more innovation in making the electronics and devices used in everyday human lives more and more personal and interactive. The colossal interest and research in the development of flexible and multi-functional sensors are a result of this demand. However, it is still a significant challenge to fabricate such flexible wearable devices using simple and cost-effective approaches that can be utilized in mass production or directly integrated into textile manufacturing without introducing additional complicated steps that require high-end laboratory-grade technology. This thesis addresses the issue regarding the need for a mass-producible process for developing wearable and flexible sensors by utilizing ancient technology like stencil printing that is fast, simple, and cost-effective.

In this work, a graphene/carbon black complex-based conductive ink was developed, which utilizes the filler behavior of carbon black particles among graphene sheets to enhance the electrical performance of the ink. The polymer-assisted binding using polycarbonate enabled the ink to be easily printable with desired patterns with excellent adhesion and stability. First, a functional tattoo capable of sensing different pressure levels was developed, which works by utilizing the change in capacitance of a two-dimensional printed capacitor with the change of pressure. An interdigitated comb geometry was used to fabricate the capacitive sensor that increases the interactive area between the electrodes, resulting in enhanced performance of the two-dimensional capacitor. The capacitive touch sensor could differentiate among multiple pressure levels at different time ranges with fast and consistent performance. Furthermore, a stretchable textile-based strain sensor was developed with the ink on a cotton fabric substrate that can detect human motion and bending by measuring the change in resistance using

the same stencil printing methodology. The sensor was capable of detecting different levels of bending and also was able to differentiate between fast and slow bending motion. Furthermore, the textile-based strain sensor could withstand multiple washing cycles and could exhibit similar performance trends for strain sensing.

Keywords: Flexible Electronics, Printed Electronics, E-tattoo, Smart Textile, Sensors.

ÖZET

TEMAS VE GERILIM GERI BILDIRIMINE SAHIP ELASTIK BASKLANMŞ ELEKTRONIK DEVRELER

Hussain Kawsar Chowdhury
Malzeme Bilimi ve Nanoteknoloji, Yüksek Lisans
Tez Danışmanı: Fatih İnci
Ağustos 2024

Bu teknolojik devrim çağı, günlük insan yaşamında kullanılan elektronik ve cihazların daha kişisel ve interaktif hale getirilmesinde daha fazla yenilik gerektirmektedir. Esnek ve çok fonksiyonlu sensörlerin geliştirilmesine olan büyük ilgi ve araştırmalar, bu talebin bir sonucudur. Ancak, bu tür esnek giyilebilir cihazları, kitlesel üretimde kullanılabilecek veya yüksek kaliteli laboratuvar teknolojisi gerektiren ek karmaşık adımlar gerektirmeyen basit ve maliyet etkin yaklaşımlar kullanarak üretmek hâlâ önemli bir zorluktur. Bu tez, stencil baskı gibi hızlı, basit ve maliyet etkin bir teknoloji kullanarak kitlesel üretime uygun esnek ve giyilebilir sensörlerin geliştirilmesi ihtiyacını ele almaktadır.

Bu çalışmada, karbon siyahı parçacıklarının grafen tabakaları arasında dolgu malzemesi olarak davranmasını kullanarak mürekkebin elektriksel performansını artıran, grafen/karbon siyahı kompleksi bazlı bir iletken mürekkep geliştirilmiştir. Polikarbonat kullanılarak yapılan polimer destekli bağlama işlemi, mürekkebin istenilen desenlerle kolayca basılabilmesini ve mükemmel yapışma ve stabilite sağlamasını mümkün kılmıştır. İlk olarak, farklı basınç seviyelerini algılayabilen fonksiyonel bir dövme geliştirilmiştir. Bu dövme, basınç değişimi ile iki boyutlu bir kapasitörün kapasitansındaki değişimi kullanarak çalışır. Kapasitif sensörün performansını artıran, elektrotlar arasındaki etkileşim alanını artıran interdigitated tarak geometrisi kullanılmıştır. Kapasitif dokunmatik sensör, farklı basınç seviyelerini farklı zaman aralıklarında hızlı ve tutarlı performansla ayırt edebilmiştir. Ayrıca, pamuklu kumaş altlık üzerinde aynı stencil baskı metodolojisi kullanılarak insan hareketi ve bükülmeyi algılayabilen esnek bir tekstil tabanlı gerinim sensörü geliştirilmiştir. Sensör, farklı bükülme seviyelerini tespit edebilmiş ve ayrıca hızlı ve yavaş bükülme hareketleri arasında ayrım yapabilmiştir. Dahası, tekstil tabanlı gerinim sensörü birden fazla yıkama döngüsüne dayanabilmiş ve gerinim algılama için benzer performans eğilimleri sergileyebilmiştir.

Anahtar sözcükler: Esnek Elektronikler, Baskılı Elektronikler, E-dövme, Akıllı Tekstil, Sensörler.

Acknowledgement

I extend sincere gratitude to my advisor, Dr. Fatih Inci, whose guidance and encouragement have been indispensable throughout my journey. His insightful feedback and unwavering support have been my weapon in fighting challenges. I am sincerely grateful for his mentorship and the confidence he has shown in my abilities.

I am thankful to the members of our group. they have been an irreplaceable part of my life with their friendship and support. Not to mention their advice and motivation during difficult times, not to mention their help with academic work, be it discussing a problem or learning a new skill. I must thank Dr. Özgecan Erdem for her guidance, even for this thesis. I am sincerely thankful to Eylül Gülşen Yılmaz and Murat A. Güngen for their help in experiments. I would like to thank Kutay Sağdıç and Yusuf Aslan for just being themselves.

I am deeply thankful to the National Nanotechnology Research Center-UNAM for the conducive academic environment and state-of-the-art research facilities. I gratefully acknowledge the engineers and technicians from UNAM for their technical support and expertise. I would like to thank Dr. Hilmi Volkan Demir, Dr. Mustafa Ordu, and members of both their groups for their generous support in providing access to electrical characterization equipment. Also, I am thankful to Cafer Gilol for his help with characterization.

Financial support fromTürkiye Sağlık Enstitüleri Başkanlığı (TÜSEB) is gratefully acknowledged. This support has provided essential resources and opportunities that have enabled me to conduct in-depth research, and advance my academic career.

I would also like to thank the thesis committee, Asst. Prof. Dr. Aykut Erbaş and Prof. Dr. Fatma Yılmaz for the guidance and support in my thesis. Their expertise and insights have significantly enriched this thesis.

I am deeply grateful to my parents for everything I have and every opportunity

I have. They are the ones who made me who I am today. I am thankful to everyone, my friends, my family, their support has been and will always be with me and I am indebted to them for that.

Contents

List of Figures

List of Tables

Chapter 1

Introduction

1.1 Introduction

The technological revolution of the current transformative era is unfolding exponentially and changing human lives through unprecedented innovation. The recent advances we are witnessing in wearable electronics and flexible technology exemplify such a spirit of innovation. Flexible electronics have been paving the way for not only manifesting new technologies but for reinventing conventional ones into more personalized, efficient, and sustainable solutions, integrating them seamlessly with the fabric of our everyday lives.

Flexible electronics has started to put its mark in fields like health technologies, wearable sensors, implantable devices, actuators, and so on. Technology such as artificial self-healing e-skin, flexible tactile and strain sensors, wearable biosensors, and human-machine interfaces have already been such inventions and are now being improved (Figure 1.1) [1–8]. However, these also brought forth a great many challenges simultaneously due to the exponentially growing demands of improved technology with more improved functionality. It is the demand of time now for flexible electronics to have outstanding mechanical deformability and stable performance along with having a broad range of functionalities required

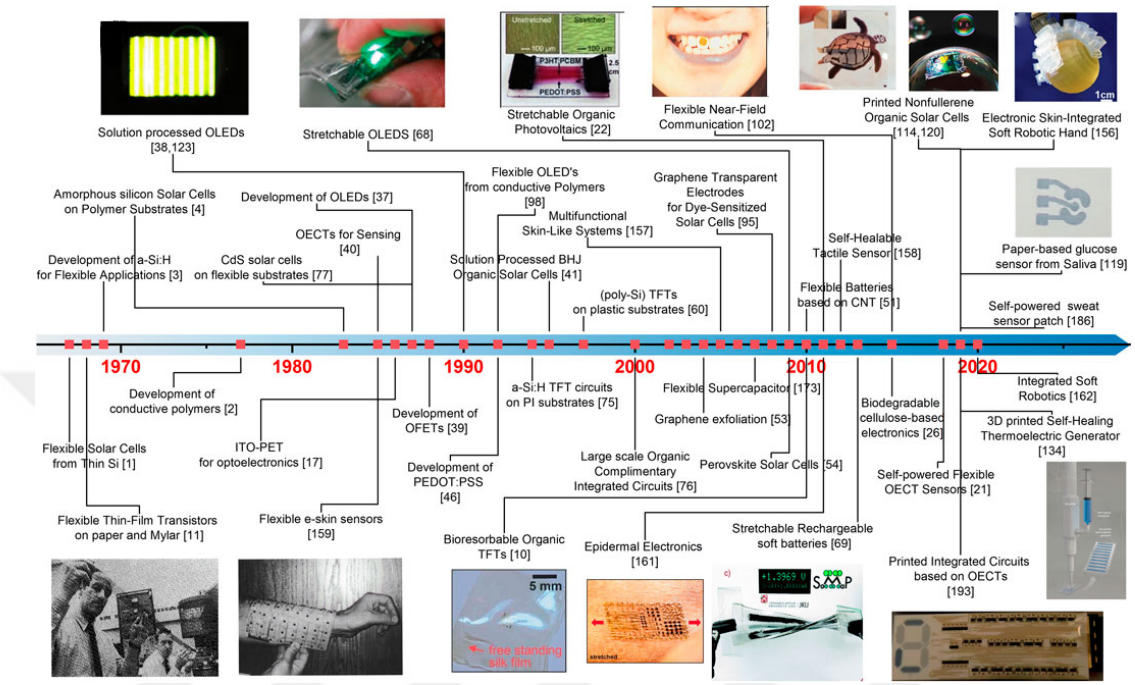

Figure 1.1: Recent development trends in flexible electronics [9].

by the diversified application markets.

The challenge of having functionality and durability while accommodating the flexibility in modern technology now makes it essential to explore new materials and approaches and overcome the limitations of conventional methodologies. Furthermore, we also have to consider their effect on human users and the environment.

Polymers are considered one of the most promising genres of materials as candidates for flexible wearable technology. Polymers exhibit a versatile range of properties, and the structures of the polymers can be designed and altered using physical and chemical manipulation to originate desired properties or even combined with other materials, such as polystyrene-based block copolymers, polyethylene terephthalate (PET), or polyimide with different sets of properties, to develop composites [10–13]. They are readily available and can be processed with convenient, cost-effective methods. Furthermore, many polymers, such as polydimethylsiloxane (PDMS) or PET, have excellent biocompatibility, and that can

be significantly advantageous in such applications as flexible technology, where the electronics are designed to directly be in skin contact or even implanted in the human body [13–16].

Consequently, polymers have become an essential element in developing flexible electronics. Polymers like PET, PDMS, and polyimide can serve as flexible substrates for conductive materials to develop electronics; they can be the binder attaching the components to the substrate, or they can even act as protective encapsulants [14,17–21]. Polyimide has been used in developing ultrathin bendable solar cells [22]. A polystyrene-block-poly(ethylene butylene)-block polystyrene (SEBS)-based composite film has been used to develop electronic skin capable of sensing temperature and touch [23]. Many other polymers can also act as the main active material in developing the technology. For example, conductive polymers, such as poly(3,4-ethylenedioxythiophene): poly(styrenesulfonate) (PEDOT:PSS), polyaniline (PANI), polypyrrole (PPy), have been implementing in developing flexible technology for their tunable electronic properties due to their -conjugated structures [24–27]. PPy particles were dispersed in an elastic supramolecular polymer matrix to develop a strain sensor capable of monitoring human motion [28]. However, inorganic materials have been reported to exhibit superior electrical properties and charge transport. Carbon materials, which have the honeycomb-resembling structure of crystal lattice with carbon atoms forming sp2 bonds, for instance, carbon nanotubes (CNTs), graphene, and carbon black, have been a significant part of developing flexible technology due to their special microscopic structure, enabling them to have low density and high strength along with excellent conductivity and excellent flexibility [29–31]. For instance, graphene is a two-dimensional crystalline allotrope of carbon, where the carbon atoms are closely packed in a well-ordered pattern, and such a structure consequently results in good electrical conductivity, which has been used in developing flexible technology like electronic tattoo sensors [32,33]. Besides, materials like carbon black, a microcrystalline layered array of condensed carbon rings with randomized orientations, have also been reported to be used to develop flexible strain sensors or conductive inks for fabricating flexible electronics, which, even though has a lower conductivity than graphene, are relatively cost-effective

[34–37].

1.2 Approaches in Flexible Electronics

1.2.1 Conductive Ink

Conductive inks have been a significant part of the development of flexible devices. They consist of conductive elements (like metal particles, carbon materials, or conductive polymers) and binding material for adhesion of the functional materials on the substrate, suspended in an appropriate liquid medium [38]. They gained a lot of attention in this field because they make it possible to take many convenient and simpler fabrication methodologies with low wastage into consideration, for example, inkjet printing, stencil printing, screen printing, or even dip coating (Figure 1.2) [39–44]. Moreover, the wide range of possible materials and combinations, such as different polymer binders like polyvinylidene fluoride (PVDF) with good mechanical properties or silicon rubber with good stretchability, along with metal derivatives like silver nanoparticles with higher conductivity, or carbon materials like graphene with higher flexibility make conductive inks remarkably versatile when it comes to achieving different properties [40,45–50].

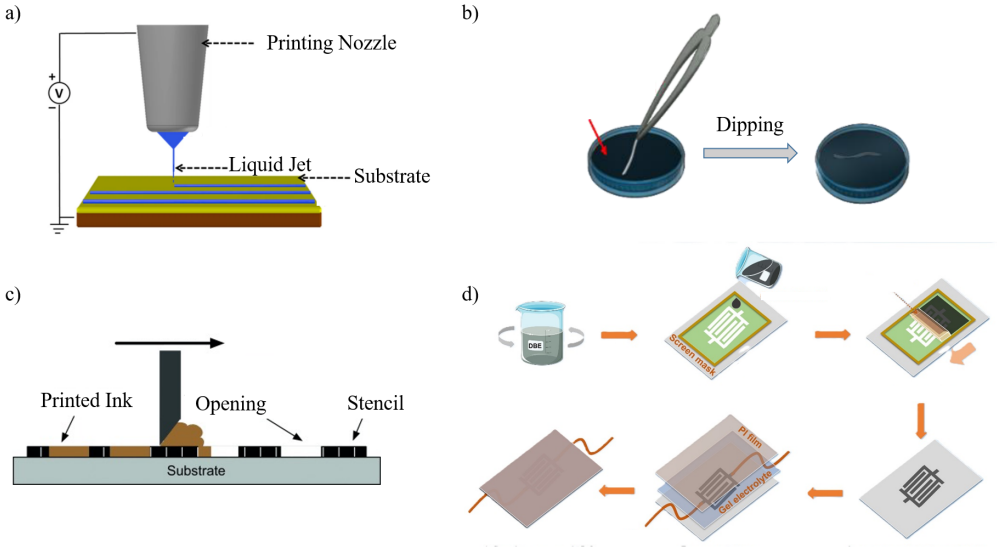

Figure 1.2: Schematic representation of (a) inkjet printing, (b) dip coating, (c) stencil printing, and (d) screen printing [41–44].

Metals (i.e., gold and silver-based inks) have been reported to be used for flexible electronic device fabrication using methods like inkjet printing to take advantage of their excellent high conductivity [39,51,52]. However, along with being highly expensive, the low content and electromigration behavior of silver is a big disadvantage in using silver inks in large-scale manufacturing. Copper was also considered due to their low cost, yet comparable conductivity [53,54]. However, they can easily get oxidized ending up with decreased conductivity [40]. On top of that, high sintering temperature is another limiting factor with metal-based conductive inks when using flexible substrates like polymers, textile yarns and fabric, and paper [55]. Carbon-based materials show great potential in this prospect. They are highly reputed due to not just their high electrical and thermal conductivity, they have good chemical inertness, and consequentially show good potential to be used with a wide range of electrolytic aqueous solutions with considerable stability [56,57]. Graphite, the prevalent form of carbon, has been reported to be used in making conductive inks due to their wide availability at high purity and low cost; they did show potential in developing flexible electronics

and good stability in different pH solutions [58]. However, although more expensive, other advanced carbon-based materials like graphene, CNT, carbon black, and so on, bring outstanding improvements in the overall analytical performance due to their much higher conductivity (both thermal and electrical), larger active surface area, and formidable mechanical strength [40,59]. Graphene and carbon black ink were printed using inkjet printing and screen-printing to produce highly conductive electrodes on paper as flexible substrates, and the possibility of applications like the development of pressure and strain sensors was demonstrated [60–63].

1.2.2 Electronic Tattoo

Skin is not just the protective layer of our body; it is also a sensitive interface that carries out information about the physical and chemical situation in our body and also exchanges materials between our body's internal environment and the external environment, be it through perspiration or enabling us of the sense of touch [64–67]. Skin holds a plethora of sensory receptors, which are responsible for detecting different internal and external stimuli, such as strain, bending, pressure, or vibration. They can detect changes in temperature, differentiate between different material states like solid and liquid, and give responses such as pain to make humans capable of perceiving and interacting with the external world. The skin can heal itself, when it is damaged due to any external influences. Through the skin, many health-related biochemical and physical data can be accessed, and therapeutics can be administered [65].

Being inspired by these extraordinarily useful and multifunctional properties of skin, scientists started working on developing flexible electronics and devices that can replicate not just the physical properties but also the functionalities of the skin and even more. The development of on-skin functional tattoos is a brunch of these research advances and has risen as an avant-garde approach in the field of flexible technology with key prospects in the field of skin-attacable flexible electronics, robotics, and prosthetics. Such devices can be used to acquire

physiological information and deliver therapeutic stimulation and drugs to the body. Furthermore, they can be used to emulate human skin-like sensations to be used in robotics and also for people who has no choice but to use prosthetics such as artificial limbs due to unfortunate accidents.

In developing electronic tattoos as well, noble metals were first utilized at first owing to their high conductivity [68–70]. A silicone layer was used as the substrate for the electronic setup made with gold to develop a multifunctional sensor for temperature, strain, and electrophysiology. Polyvinyl alcohol (PVA) was used as a sacrificial layer utilizing its water-solubility and the setup was attached to the skin based on just van der Waals force [68]. In another similar work, a commercially available tattoo paper was laminated with 1.4 µm thick PET using the water-soluble adhesive layer that was pre-existing on the tattoo paper, followed by hotplate drying at 50-60 °C for 5 minutes to prepare the substrate, where the metal electrodes would be fabricated. The metal electrodes were composed of a chromium layer with 10 nm thickness and a gold layer with 100 nm thickness on top of the chromium layer, and both of these layers were printed using a thermal evaporator. This gold/chromium/PET tattoo sensor was fabricated to measure skin hydration, skin temperature, and electrocardiogram [70]. Metal such as gold was used in developing these electronic setups due to their high conductivity. However, using metal-based electrodes has its own set of problems. They are very expensive and also do not have high flexibility. This high cost and poor flexibility of metal-based electrodes have led to the exploration of many other conductive materials and complexes with additional desired properties. Carbon materials have been used to develop functional tattoos capable of electrochemical sensing. Carbon fibers were dispersed within the tattoo ink and then screen-printed on temporary tattoo papers to be attached to the epidermis [71]. A CNT-based electronic tattoo prepared with a screen printing technique was reported to successfully monitor lactate in human perspiration. Carbon fibers were added within the conductive carbon ink and both the working and counter electrodes were fabricated using this ink. Also, the silver/silver chloride ink was mixed with carbon fibers in the same way to develop the reference electrode. This carbon fiber doping resulted in improved tensile strength. Lactate

oxidase was used to functionalize the working electrode for lactate monitoring [72]. Another tattoo sensor was fabricated using the same methodology of adding carbon fibers into the conductive inks and was functionalized for monitoring the sodium level in sweat [73]. Electronic tattoos are also being used in developing flexible electronics for physiological monitoring and actuators. Graphene-based tattoos fabricated with Chemical vapor deposition (CVD) have been reported; large-area graphene was grown on copper foil and then coated with poly(methyl methacrylate) (PMMA) that had a thickness smaller than a micrometer with the purpose of etching the copper layer. The copper-etched graphene/PMMA layer with a sheet resistance of 1994.33 $\pm$ 264 Ω/sq was then transferred on tattoo paper for skin mounting, and the developed sensor was used to monitor ECG, EMG, EEG, and skin temperature [74,75]. CNT-based tattoos have also been developed for capacitive tactile sensing [76,77]. PVA was used as the substrate to grow the CNT array as the electrodes using CVD and porous silver nanowire/PVA Nanocomposite Hydrogel was grown with a combined approach of foaming and freezing-thawing as the dielectric. The CNT/PVA electrodes were attached to the silver nanowire/PVA dielectric, and 10 wt% PVA solution was also utilized as the hydrogel binder to attach the CNT/PVA electrode layers to both sides of the silver nanowire/PVA dielectric in order to develop a three-dimensional capacitive tactile sensor [77].

1.2.3 Electronic Textile

Textiles are widely used in our everyday lives, so much so that they can be addressed as a secondary skin for humans. In addition, they are already developed with qualities such as breathability and flexibility to comfortably conform to the body shape. The primary goals in developing textile products are protecting our bodies from the effects of the external environment, along with aesthetics and fashion [78].

Substrates that are flexible and stretchable and possess the biocompatibility to be used in direct contact with human skin have always been a challenge in

developing flexible electronics. Textiles have the necessary flexibility, compatibility, and comfortability for direct contact use, and they are already a necessary part of our daily lives [79,80,80–87]. Therefore, they can be excellent substrates if can be utilized in developing wearable technology. By integrating textile yarns and fabrics in developing wearable technology, it is possible to improve an everyday product by adding a wide variety of functionalities, avoiding the necessity of using additional mounting of equipment to achieve the same functionalities [88–92]. Furthermore, they are low-cost and have excellent biocompatibility and biodegradability, which will take us another step forward toward sustainable electronics development [84,93–97]. Additionally, utilizing different fabric structure designs and manufacturing techniques can also complement the procedure of generating a wide spectrum of desired mechanical and electrical properties [98,99]. From this thought, began the approach towards the research and development of electronic textiles (E-textiles).

In the beginning, electroless silver and nickel plating or atomic layer deposition on synthetic and natural fibers was reported to be used to develop conductive fibrous materials for e-textiles [81,100]. Polyester fabric was first plasma treated for 10 minutes to grow active hydrophilic groups on the surface, and then Al-doped zinc oxide was grown on the active fabric surface using atomic layer deposition at 150 °C to develop conductive textile material for motion sensing [81]. Thermoplastic polyurethane nanofibers were electrospun to develop a textile substrate for inkjet printing a silver particle-based composite ink for electromyography [84]. However, this involved both expensive materials and complicated methodologies, and furthermore, showed poor endurance towards mechanical deformation. Similarly, using aluminum required the use of vacuum deposition, another expensive method, or it required an approach like depositing aluminum precursor and then decomposing it to aluminum with complicated post-treatment [101,102].

Conductive inks or dyes can be a simple and useful solution to this by utilizing faster, easier, and low-cost methodologies like screen printing, inkjet printing, or even dip-coating [103]. A conductive ink with silver fractal dendrites as the functional material and water as the dispersing solvent was reported to be screen-printed on a textile substrate for motion and temperature detection. However,

the printed ink had to be coated with a waterproofing protective layer [86]. Since washing is an essential part of textile products, scientists have also attempted to develop textile fibers that are intrinsically conductive. Multiwalled CNT, chitin carbon, and silk fibroin were mixed together and electrospun to develop silk-based conductive fibers. The fibers were used to make yarns and a flat spiral coil was sewn into textiles to develop a magnetic resonance coupling-based flexible power source for electronics [87]. Also, MXene was incorporated with PVDF to develop MXene-doped PVDF functional nanofibers through electrospinning in order to develop sensors capable of detecting tactile feedback [95]. Screen-printing of MXene-based conductive ink on nonwoven rayon fabrics has also been reported to develop capacitive pressure sensors. However, since MXene nanosheets have a tendency to oxidation, PEDOT: PSS also had to be integrated into the fabrication process to increase the stability of the sensor for long-term use [94].

Carbon material-based conductive inks have also grabbed much attention, and rightfully so. They have excellent mechanical and electrical characteristics and stability. A conductive ink was formulated, in which graphite was the functional material, PVDF polymer was the binding material, and N-methyl-2-pyrrolidone (NMP) was the solvent for the ink. This graphite/PVDF ink was used to modify a polyester/viscose fabric using a simple dip and dry method, where the fabrics were dipped into the ink for 42 hours at room temperature and then dried at 180 °C for one and a half hours to fabricate conductive fabric electrodes [103].

Functional textiles modified with conductive inks have been reported to be successfully used in applications like human posture recognition and breathing and ECG monitoring [63,104,105]. A carbon black-based composite ink was printed on textile fabric using a double screen-printing technique for recognizing human posture through strain sensing. The fabric was printed with the prepared ink, dried at 100 °C for 1 minute, then printed again, and finally dried for an hour at 100 °C [104]. In another work, a cotton fabric was modified by heat printing an adhesive transfer paper to develop the substrate for a graphene/CNT composite ink to develop strain sensors. The ink was first screen-printed on the substrate and then subjected to compression rolling for a more firm attachment and better performance [105]

Chapter 2

Flexible Human-Machine Interfaces

2.1 Introduction

Three interrelated terms can be used to explain the concept of human-machine interface for our study: transducers, sensors, and actuators. Transducers are tools that convert energy from one form to another [106,107]. Sensing systems or sensors are devices capable of detecting different physical stimuli, such as heat, light, pressure, sound, and motion, or even biological and chemical components, and quantifying them by converting them to electrical signals [108–111]. Actuators convert a signal, which is usually electrical, to another action, such as any type of mechanical output [112–114]. Therefore, in simple words, sensors and actuators can both be considered forms of transducers, where sensors perform a transducing action to detect and quantify physical stimuli or biological and chemical components; on the other hand, actuators also perform sensing but to activate another type of action.

2.2 Types of Sensors

Mechanical Sensors: Mechanical sensors work by detecting different types of deformation and deflection of materials or friction on materials and then converting them to electrical signals. Mechanical stimuli such as acceleration, stress, pressure, and bending of materials, even the position and angle of substances placed on the sensor, or the flow rate of substances are measured using such sensors [115–119]. Flexible mechanical sensors have been of great interest to scientists for a while due to their potential in the field of healthcare and sports analytics, and many routes and approaches were taken in order to develop such sensors. Fabrication of conductive hydrogels has been reported to develop flexible strain sensors [120]. To enhance the mechanical properties of hydrogels, nanocomposite hydrogels and cross-linked hydrogels have been attempted [121–123]. A carbon material-based flexible strain sensing device has been developed by mixing carbon materials with PDMS and Ecoflex [124]. Textile materials have been used as flexible substrates for both strain sensing and pressure sensing [125,126]. Different principles such as piezoresistivity and capacitance have also been reported in developing mechanical sensors, for instance, pressure sensors, by utilizing a wide range of materials like conductive polymers and carbon-based materials [127]. 3D printing has been utilized in recent times as well in order to develop flexible mechanical sensors [128].

Optical Sensors: Optical sensors are devices capable of detecting and measuring light or optical signals and converting these optical signals into electrical signals or other forms of output [129–133]. From chemical detection in laboratories to point-of-care biosensors, even in the field of robotics and actuators, optical sensors have been used for many different applications [134–136]. An example of an optical sensor can be a conventional and simple colorimetric sensor that can detect a material or chemical with the change of color, for example, a litmus paper, or can also be a fluorescent sensor that precisely quantifies the fluorescent spectra to identify an analyte with excellent sensitivity and selectivity [134]. A fluorometric approach has also been reported to be used in developing sensors

capable of detecting changes of pH in solutions in real-time, which can be a useful marker in not just guiding and maintaining chemical interactions but also preventing many serious physiological problems, for instance, Parkinson's disease [137]. Another well-known principle used in developing optical sensors is surface plasmon resonance (SPR). It is a phenomenon that happens when plane-polarized light hits a metal surface with full internal reflection, causing electron oscillation. SPR exhibits a direct relation with the refractive index of the medium, and this relation is used to develop SPR sensors [138]. SPR sensors have been widely used in identifying different biomolecules, even cancer biomarker detection [139]. Optical sensors have also been reported in developing flexible tactile sensors using optical microfibers and could differentiate between different tactile feedback from the intensity change of transmitted light [135].

Thermal sensors: Thermal sensors work by using the change that occurs in materials as their temperature change. The change can be quantified by converting it into electrical signals, and a digital thermometer can be a simple example of a thermal sensor [140–143]. Body temperature is a crucial physiological parameter, and many attempts have been made to develop flexible thermal sensors capable of continuous thermal monitoring of the human body [144]. The temperature dependency of the electrical resistance of metals like gold and silver, carbon materials like graphene and CNT, and conductive polymers such as PEDOT: PSS and polypyrrole has been used to develop flexible temperature sensors [144]. Also, materials like silver, graphene, or CNT have been used to develop inks, which were printed on flexible substrates using different processes like inkjet and screen printing [60,145,146]. A flexible thermal sensor was also reported to use polyacrylamide/carrageenan hydrogel, which could improve the sensitivity from 2.95 to 19.6% / °C by partially substituting the water content with small-molecule polyols [147].

Acoustic sensors: These types of systems detect and measure acoustic signals like sound waves and convert them into electrical signals [148–151]. Acoustic sensors have been in the field for a long time and have been used in determining the velocity, position, and distance of materials, even underwater, used to detect icebergs and submarines [152]. Implementing an acoustic sensing system

in wearable electronics could be used to detect changes in acoustic properties, and this principle can be utilized in a broad spectrum of applications. Flexible skin-attachable piezoelectric acoustic sensors have been utilized for applications like sound detection and speech processing [148,153]. In another work, a surface acoustic wave-based sensor was developed that utilized the larger surface area of zinc oxide nanowires and hydrophilic functional groups of graphene quantum dots to achieve ultrasensitive humidity sensing [154]. Acoustic sensors have also been utilized as diagnostic tools and reported to be used for point-of-care sensing and removal of nonspecifically bound proteins [155,156].

Biological and Chemical Sensors: These types of sensors can detect biological and chemical interactions and convert them into electrical signals for quantification [157–166]. Electrochemical sensors can be the perfect example of such sensors. These sensors consist of a functionalized surface with a recognition element for the target chemical or biomolecule, which is in contact with an electronic setup for sensing the chemical or biochemical reaction happening on the active surface and converting it into a quantifiable electrical signal [167,168]. Many flexible electrochemical sensors have been reported to be developed for detecting different biomarkers in sweat and blood [63]. An electrochemical sensor with gold nanomembrane-based electrodes on a bioresorbable substrate has been developed capable of nitric oxide detection in the joint cavities [169]. In another work, an electrochemical sensor was developed by fabricating the electrodes with screen-printing to detect pH change and lactate in sweat [170].

In this study, we have used mechanical sensors capable of detecting and measuring pressure and angular bending through changes in electrical signals (capacitance and resistance, respectively).

2.3 Capacitive Touch Sensors

Capacitance is the quantification of the ability of a system to store electrical energy as electric charge form. In a basic capacitor setup, there are two conductive plates and they are separated by a dielectric component. When a voltage is applied across the plates, one of the plates becomes negatively charged, and the remaining plate becomes oppositely charged. Due to this charge separation, an electric field is generated between the plates through which energy is harvested in the capacitor (Figure 2.1 (a)). Using equation (2.1), the capacitance of parallel plate capacitors is theoretically calculated [171],

$$C = \varepsilon_0 \varepsilon_r \frac{A}{d} \tag{2.1}$$

Here,

ε_0 = absolute dielectric permittivity

ε_r = relative permittivity of the used dielectric material

A = surface area of the used plates

d = the distance between the plates

However, the electric field does not only work between the electrodes (plates) but surrounding the plates. Based on that principle, two-dimensional (2D) co-planar capacitors can be produced, and the capacitance of such systems can be tuned through alteration of the relative permittivity of the system by introducing new elements on the dielectric surface. This concept is useful in developing capacitance-based touch sensors capable of measuring the pressure inflicted through touch (Figure 2.1 (b)).

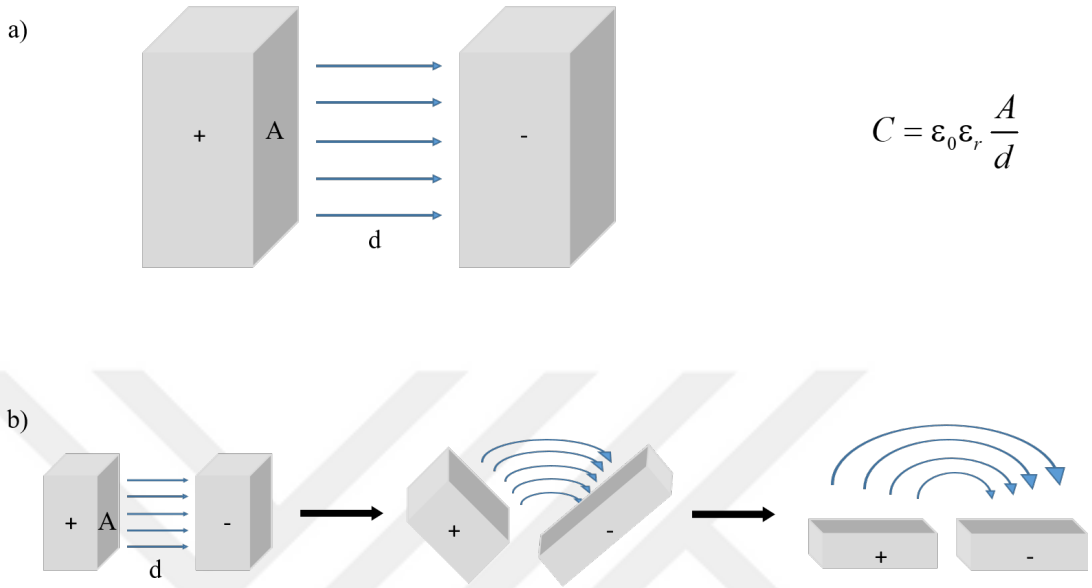

Figure 2.1: The schematic representation of (a) a basic parallel-plate capacitive setup and b) the evolution of electric fields with the transition of a parallel plate capacitor to a co-planar capacitor.

The comb-structured capacitors, known as interdigitated capacitors, are a more complex version of these 2D capacitors made to improve capacitive performance with enhanced efficiency (Figure 2.2). Equation (2.2) can be used to calculate the theoretical capacitance values for interdigitated capacitive sensors [172,173],

$$C = \varepsilon_0 \frac{(\varepsilon_r + \varepsilon_k)\, K\left(\sqrt{1 - \left(\frac{a}{b}\right)^2}\right)}{K\frac{a}{b}} + 2\varepsilon_0 \varepsilon_k \frac{t}{a} \tag{2.2}$$

Here,

ε_0 = absolute dielectric permittivity

ε_r = relative permittivity of the substrate

ε_k = relative permittivity of the dielectric film

a = width of the electrodes

b = spacing between two adjacent electrodes with the same charge

t = thickness of the electrodes

K = complete elliptic integral of the first kind

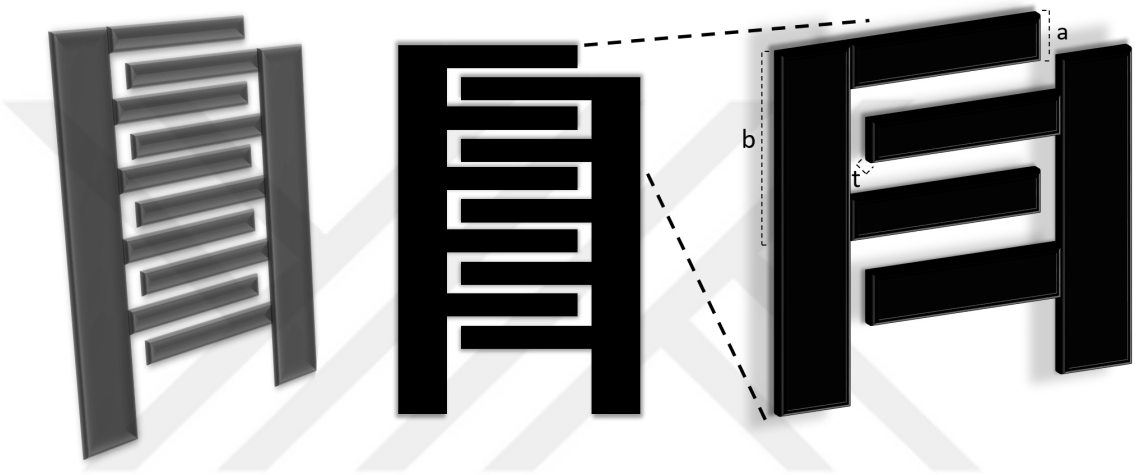

Figure 2.2: Schematic diagram of an interdigitated capacitive system.

Moreover, experiments have revealed that the capacitance of an interdigitated sensor is positively affected by the increment of the length and width of the fingers in the comb structure because it increases the surface area, while it is inversely affected by the distance between two fingers or electrodes due to the weakening of electric field between them [173]. Also, the number of fingers or electrodes can be increased to increase the overall effective area of the capacitance, which consequently results in enhanced capacitance [173].

2.4 Resistive Strain Sensors

The electrical resistance of a material is the property that quantifies how much opposition flow of current will face through this material. If we consider a basic rectangular block, then equation (2.3) can be used to calculate the theoretical resistance of that cylinder [174],

$$R = \frac{\rho L}{A} \tag{2.3}$$

Here,

ρ = resistivity of the substance

L = length of the block

A = surface area of the block

So, for a certain material, changing the dimensions of the block will result in a change of resistance, and the resistive strain sensors are developed based on this theory. If we can develop a flexible, stretchable material with a specific resistance, stretching or compressing the material will cause a change in the resistance because of the dimensional changes.

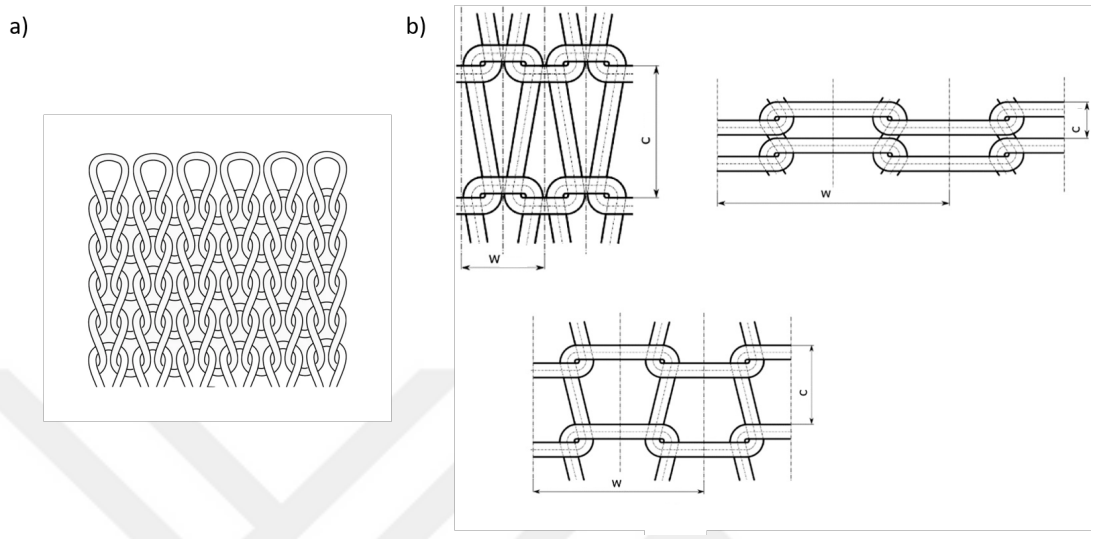

Figure 2.3: Schematic of the complex yarn network in (a) nonstretched and (b) stretched knit fabric [175].

Textile fabrics (i.e., stretch knitted fabric) are composed of complex yarn networks and can be utilized as a stretchable material. When stretching or compressing the fabric in the horizontal (W) or vertical (C) direction, the yarns get further or come closer, enforcing changes in the network (Figure 2.3) [175]. Therefore, if the fabric is coated with conductive material, the conductive pathway will change, consequently changing the resistance as a result.

2.5 The Aim of this Study

This research aims to create flexible electronic tools using polymer-assisted conductive dye capable of detecting the sense of touch and motion, which holds promise in enhancing the functionality of prosthetic limbs by enabling them to mimic sensory feedback.

A carbon material composite-based conductive ink was fabricated. The synergistic effect between the sheet structure of graphene nanoplatelets and the particle structure of carbon black was utilized in developing the composite ink to enhance its electrical properties. Carbon black was exhibited acting as a filler material between graphene sheets, which increased the electrical conductivity of the ink. Thermoplastic polycarbonate was used as the binder for the conductive ink due to its thermal stability, adhesive properties, and easy processibility. The polycarbonate binder was dissolved in dichloromethane to prepare the binder solvent. Dichloromethane is a volatile, non-flammable solvent that is capable of dissolving polycarbonate. On top of that, dichloromethane is easily evaporated at room temperature, making it easier and faster to prepare the conductive ink-based printed electrodes without any additional high-temperature curing step.

Then, carbon black was dispersed into the solvent, followed by the blending of graphene nanoplatelet. This addition sequence was maintained for better stability of the ink. Carbon black is readily dispersible in solutions. However, graphene has a tendency to restack and agglomerate in solution. This agglomeration behavior of graphene is an obstacle to formulating a homogenous solution, hindering the performance of the prepared conductive ink, and also is a problem for the stability of the ink, especially to be usable for a longer time. Therefore, in this study, we disperse the carbon black particles into the solution first, which assists the dispersion of the graphene nanoplatelets added later, along with improving the electrical performance of the ink.

The limb movements were detected using a flexible strain sensor through the change of resistance with changing strain. Textile fabrics were chosen as the

flexible medium because of their flexible and stretchable properties. In addition, they are already an integral part of our everyday life. Furthermore, the knitted structures of textile fabrics create complex conductive networks that can have a remarkably positive impact on the change of resistance in the system when physically altered, and that is complementary to developing a stretchable strain sensor. For this study, an untreated cotton knit fabric was used. Cotton is a natural fiber that is cost-effective, easily available everywhere, and very comfortable. Furthermore, it is one of the most used fibers in textile industries to develop apparel products. So, functionalizing cotton-based fabric would be a notable step toward the commercialization of textile-based functional devices. A similar stencil-printing approach was implemented in developing the textile-based strain sensor. A patterned adhesive stencil was attached to the fabric first. Then, the prepared ink was applied to the pattern. After drying the pattern for 30 minutes, the stencil was removed from the textile fabric, and the fabric-based resistive strain sensor was prepared. If a dyeing process such as this can be utilized in functionalizing textile yarns and fabrics, then we will have simple methodologies to develop e-textiles, nullifying the requirements of additional processes, and will be able to directly integrate the functionalization process of textiles to the general manufacturing protocol.

With changing strain, the yarn network of the yarns inside the fabrics altered, which changed the resistance of the sensor because the conductive pathway was changed as a result of the fabric deformation. With increasing strain, a decrease in the resistance value for the strain sensor was observed, and alternatively, with decreasing strain, an increase in the resistance was observed. This happened because when the textile fabric was not stretched, it maintained its relaxed knit structure with periodic connections with air gaps in between the yarns in the fabric, which was the reason behind the lower resistance observed in the fabric. However, when the conductive fabric was stretched, the yarns in the fabric became parallel lines in full contact with each other with no gaps, which resulted in a decrease in the resistance of the fabric. And, with more stretching, the yarns came more in contact with each other with smaller to no gaps, resulting in a decreasing trend in the resistance. After the stretching was removed, the fabric went back

to its previous relaxed structure resulting in an increase of the resistance again.

Chapter 3

Materials and Methods

3.1 Materials

Graphene nanoplatelet (Gr) (Purity: 99.9 %, Size: 5 nm, S.A:800 m^2 /g , Dia: 18 m), and Carbon Black (CB) (Purity: 95%, Size: 148 nm) were purchased from Nanografi. Polycarbonate (PC) was obtained from Ajedium films. Dichloromethane (DCM) (Puriss, Molecular Weight: 84.93, NF, 99% (GC)) was obtained from Sigma-Aldrich. Commercially available temporary transfer tattoo paper (SRF LaserTattoo), commercially available detergent for washability test, and untreated cotton fabric were obtained from local suppliers.

3.2 Conductive Dye Formulation

PC film was dissolved in DCM to prepare the PC binder solution with a concentration of 50 mg/ml. 40 mg/mL CB was dispersed into the prepared PC-based liquid medium and mixed with a vortex mixer for 1 minute.

Afterward, Graphene nanoplatelets were added to the blend with a concentration of 30 mg/mL in DCM/CB complex solution and mixed again for 1 minute.

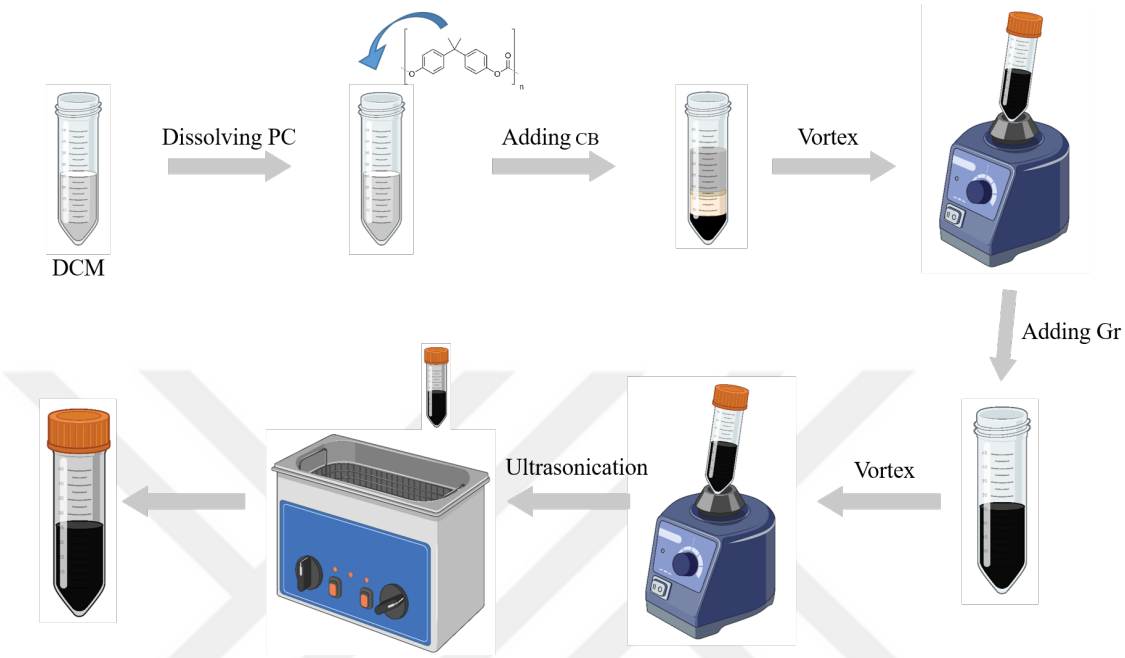

Figure 3.1: Schematic of the conductive dye preparation method.

Finally, the solution was ultrasonicated for 10 minutes to ensure the homogenous distribution of all the components in the solvent.All the steps during the conductive dye preparation were done at room temperature (Figure 3.1).

3.3 Sensor Fabrication

3.3.1 Capacitive Touch Sensor Fabrication

Fabrication of the functional tattoo for capacitive touch sensors was done by stencil printing of the CB/Gr conductive ink. Commercially available tattoo paper was used as a simple and copiously available substrate for the ink. The tattoo kit has two components: a decal transfer paper and a double-sided adhesive sheet. The ink was printed onto the decal transfer paper, while the adhesive layer was used to attach the sensor to the skin and also as the insulating passivation layer, that keeps the electrodes separate from the skin.

An adhesive stencil-printing frame was prepared with the required comb-structured pattern for printing the interdigitated electrodes for the capacitive touch sensors using a 30-watt Zing 16/24 CO_2 laser cutting and engraving system. This printing frame was attached to the decal paper. The conductive ink was dispersed on the patterned frame, and then the ink was dried for 5 minutes at room temperature. After that, the patterned frame layer was removed to obtain the comb-structured electrodes for the interdigitated capacitive sensors. The fingers of the combs have a length of 6mm and a width of 1.5 mm. The distance between the adjacent opposite electrode fingers is 0.5 mm. Finally, the adhesive sheet of the tattoo paper was used to attach the tattoo to the subject (Figure 3.2).

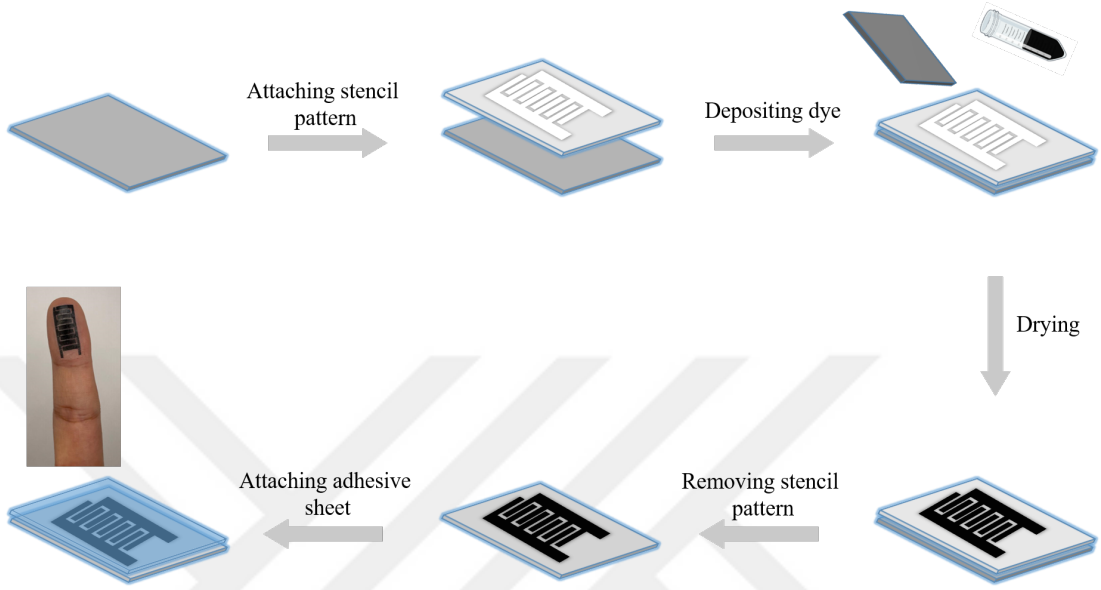

Figure 3.2: Schematic of the capacitive touch sensor tattoo fabrication process.

3.3.2 Resistive Strain Sensor Fabrication

To fabricate the textile-based strain sensors, untreated stretchable knit cotton fabric was used. First, the fabric was washed using distilled water and dried at room temperature. The adhesive printing frame prepared with a 30-watt Zing 16/24 CO_2 laser cutting and engraving system was then placed on the washed cotton fabric. The prepared conductive ink was then coated on the fabric by using a facile printing process (Figure 3.3). After that, the conductive fabric was allowed to dry for 30 minutes at room temperature. Finally, the fabric was attached to the joints of the subject for human physiological motion and bending recognition.

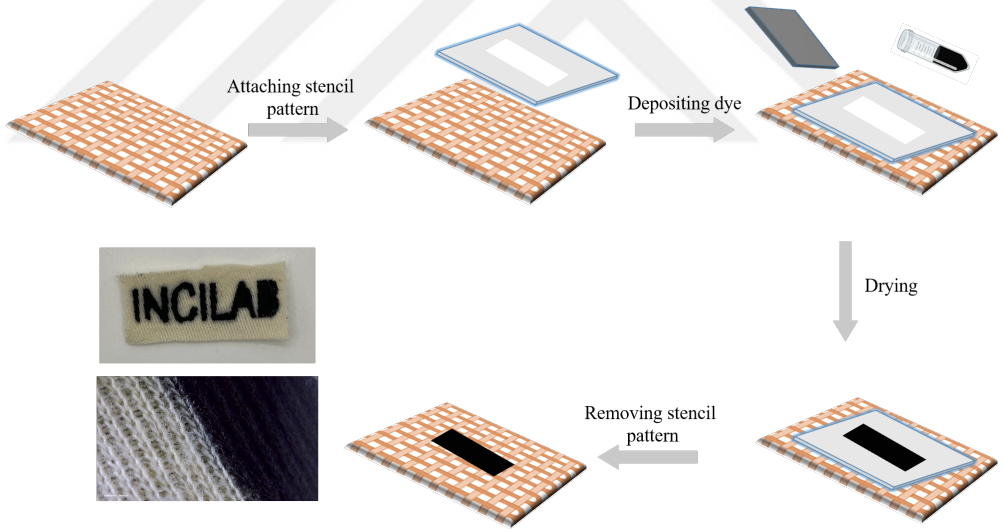

Figure 3.3: Schematic of the textile strain sensor fabrication process.

3.4 Materials Characterizations

The morphological structure and distribution of the conductive dye of the ink were investigated with multiple materials characterization approaches.

3.4.1 Raman Spectroscopy

3.4.2 Scanning Electron Microscopy (SEM)

SEM is used to produce high- resolution and depth-of-field images of micro and nanostructures by utilizing focused beams to excite inelastic scattering-induced secondary electrons [178]. In this work, SEM (Quanta 200 FEG, Field Electron and Ion Company, FEI) (Hillsboro, OR, USA) was used for observing and imaging the distribution of materials on the printed ink. Since the ink itself was conductive, there was no need for a sputtering process for the analysis.

3.4.3 X-Ray Photoelectron Spectroscopy (XPS)

XPS is an analytical method that is used to investigate the material composition and chemical state on the surface by analyzing the kinetic energy of photoelectrons, which are emitted from the sample surface upon the impact of X-rays [179]. A comprehensive XPS survey was conducted using X-ray photoelectron Spectroscopy (XPS) (K-Alpha, Thermo Scientific) (Waltham, MA, USA). The individual spectrum peaks associated with Carbon (C), Oxygen (O), and Chlorine (Cl) were analyzed. For the data analysis, the peaks were first shifted according to the C1s peak before conducting any data analysis. To determine the peak information related to different elements, a peak deconvolution method was applied.

3.5 Electrical Characterization

3.5.1 Probe Station

A probe station is an electrical characterization tool that consists of probes, making contact with the sample to apply electrical stimuli and measure the electrical properties of the sample. A two-probe measurement system was used in order to perform the electrical characterization of the samples. [180]. A Keysight B1500A Semiconductor Device Parameter Analyzer (Keysight Technologies, Inc.) (Santa Rosa, California, USA) with Cascade Alessi REL-4800 (Cascade Microtech) (Beaverton, Oregon, USA) was used to take an I-V (current vs voltage) sweep, to detect the resistance of the samples (Dimensions: 2 x 2 cm) based on equation (3.1).

$$R = \frac{V}{I} \tag{3.1}$$

Here,

R = resistance measured with the 2-probe station

V = voltage applied

I = current measured

And, equation (3.2) was used to calculate the sheet resistance of the samples [181],

$$R = R_{\mathrm{s}}\frac{L}{W} \tag{3.2}$$

Here,

R = resistance measured with the 2-probe station

L = length of the sample

W = width of the sample

3.5.2 LCR Meter

An LCR meter is an electrical equipment that is used to measure the inductance (L), capacitance (C), and resistance (R) of materials [182]. In this study, a Keysight E4980A Precision LCR Meter (Santa Rosa, California, USA) was used to evaluate the capacitance change of the capacitive touch sensor tattoo and how different amounts of pressure affect the sensor.

3.5.3 Source Meter

For this study. A Keithley's Standard Series 2400 Source Measure Unit (SMU) (Cleveland, Ohio, United States) was used to evaluate the change in resistance due to strain in the textile-based strain sensor.

3.5.4 Arduino Setup

A voltage divider circuit was prepared using Arduino UNO R3 (Ivrea, Italy) with a fixed input voltage, a known resistance, and the prepared strain sensor. A voltage divider circuit is made of two resistors connected in series. The first resistor is connected to the input voltage and the output point, and the second resistor is connected to the ground and the output point. After applying a known voltage across the series, the output is measured at the junction point of $\mathbf{R_1}$ and $\mathbf{R_2}$ relative to the ground (Figure 3.4 (a)) using equation (3.3) [183].

$$V_{\text{out}} = V_{\text{in}} \times \frac{R_2}{R_1 + R_2} \tag{3.3}$$

Here,

V_{out} = output voltage

V_{in} = input voltage

R_2 = resistor connected to the output point and the ground

R_1 = resistor connected to the input voltage and the ground

Since V_{out} is dependent on the values of R_1 and R_2, if the value of V_{out} is known, then the value of an unknown resistor can be measured with this circuit using equation (3.4), considering R_2 as the unknown resistor.

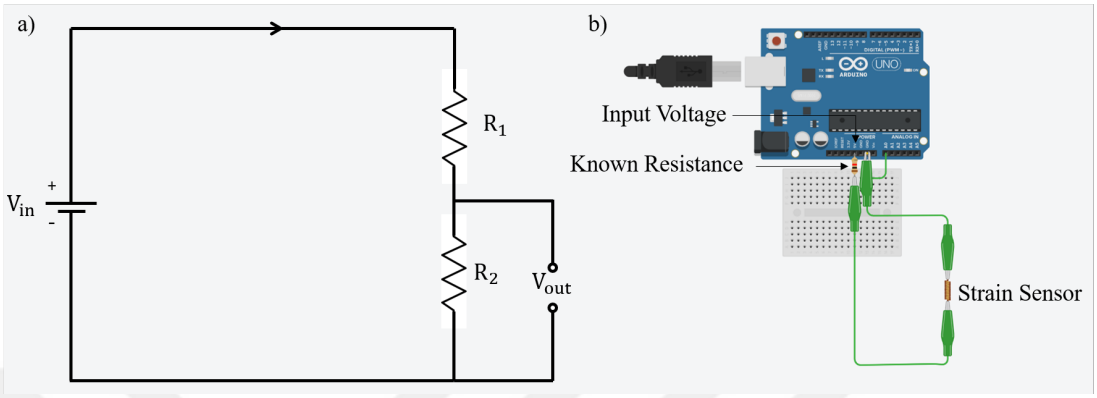

Figure 3.4: Schematic diagram of (a) a basic voltage divider circuit and (b) the Arduino setup with the strain sensor.

$$R_2 = R_1 \times \frac{V_{\text{out}}}{V_{\text{in}} - V_{\text{out}}} \tag{3.4}$$

3.6 Biological characterization

3.6.1 Cell Culture and Cell Viability

Cell viability testing is an in-vitro biological characterization methodology, where the number of live and dead cells are determined after a certain period within a sample, and it is used in applications like cytotoxicity testing and drug development [184,185]. An MTT assay with a 3T3 cell line (mouse embryonic fibroblasts) was used to determine the cell viability of the samples for 7 days. The MTT assay is a colorimetric approach to cell viability testing based on the live cell's ability to decrease the MTT (yellow tetrazolium dye) generating formazan crystals (purple) by the action of mitochondrial enzymes, particularly succinate dehydrogenase [186]. First, 3T3 cells (5 x 106 cells/well) were seeded into a 6-well plate and 48 hours of incubation was done to allow the cells to adhere to the surface and grow. After that, the samples were put into the wells and incubated for 7 days. The DMEM/F-12 (Dulbecco's Modified Eagle Medium/Nutrient Mixture F-12) medium was used for the cells. Additionally, 10% FBS, 100 U/mL penicillin, and 100 µg/mL streptomycin were added to the medium. The medium was changed every two days until the cells covered more than 85% of the surface, and after that, the passaging process was carried out.

After the cell culture process was done for 7 days, the medium solutions were removed from the wells, and each well was washed three times with a fresh medium. Then, 400 L of medium and 100 L of MTT (5 mg/mL) were added to each well, and the incubation was done at 37 °C with 5% CO_2 for 5 hours. 250 L of the medium solution was removed after the MTT incubation, and 250 L of dimethyl sulfoxide (DMSO) was added to each well to terminate further growth of cells. The plates were then incubated for 10 minutes at 37 °C with 5% CO_2. Finally, the absorbance at 540 nm wavelength was measured using a Biotek Synergy HT Microplate Reader (Hampton, New Hampshire, USA), and the cell viability percentages were calculated using equation (3.5) [187],

$$\text{Cell Viability (\%)} = \frac{(\text{Absorbance}_{\text{Sample}} - \text{Absorbance}_{\text{blank}})}{(\text{Absorbance}_{\text{control}} - \text{Absorbance}_{\text{blank}})} \times 100 \qquad (3.5)$$

Here,

$\text{Absorbance}_{\text{sample}}$ = Absorbance of the cells with samples

$\text{Absorbance}_{\text{control}}$ = Absorbance of the control cells

$\text{Absorbance}_{\text{blank}}$ = Absorbance of the blank solution

3.6.2 Microscope Imaging

To characterize the effect of the samples on cell growth after 7 days, microscopic images were taken, where the live and dead cells were distinguished using a fluorometric approach. 2 g/mL Hoechst 33342, 2 M calcein-AM, and 4 M ethidium homodimer-1 were added in a 10 mL PBS solution to prepare the dye and was applied to the cells, followed by 35 minutes of incubation at room temperature. The nuclei were stained with Hoechst 33342, live cells with calcein-AM, and dead cells with ethidium homodimer-1. Bright-field and fluorescence images of the cells were captured using a Thermofisher EVOS M5000 fluorescence microscope (Waltham, Massachusetts, USA).

3.6.3 Flow Cytometry

Flow cytometry is a characterization tool that is used to simultaneously analyze multiparametric physical and chemical characteristics of thousands of cells per second in a fluid when they pass through lasers. When the cells pass through the laser, the interaction with the laser excites the identifying components, such as fluorescent dyes attached to specific types of cells, resulting in the emission of lights with specific characteristic wavelengths, which can be differentiated from

each other [188]. In order to perform the flow cytometry in this study, the cells were detached from the surface after the 7-day incubation, and the live and dead cells were marked with Calcein AM and Ethidium Homodimer-1, respectively. A BD Accuri™ C6 flow cytometer (Becton Dickinson, USA) was utilized to corroborate the analysis of the cell viability test.

Chapter 4

Results and Discussion

4.1 Characterization

Carbon materials, especially graphene, have been an attractive choice in application fields like flexible electronics for a long time due to their wide range of appealing properties. Graphene has excellent electrical conductivity along with good mechanical properties [189,190]. However, stabilized dispersion of graphene to be able to use it in applications like formulating conductive ink has always been a challenge because it tended to restack or agglomerate [191]. On the other hand, carbon black is comparatively easier to disperse but has a lower conductivity. Therefore, recently, combining different carbon materials by utilizing the different structures of the carbon materials has been of interest to researchers to achieve a synergistic effect between them and achieve a combination of different types of properties coming from different carbon materials in the blend [192–195]. This study also aims to achieve combined properties by preparing a composite of different carbon materials.

In this study, flexible wearable sensors were fabricated by stencil printing a conductive ink. Polycarbonate was used as the binder for the conductive ink. Thermoplastic polymers like polycarbonate are cheap but have good mechanical

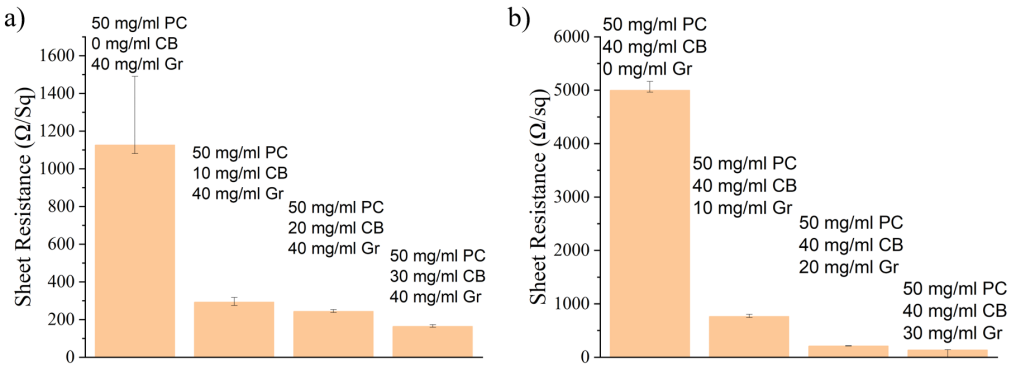

Figure 4.1: The effect on sheet resistance with changing the quantity of (a) carbon black and (b) graphene.

properties, and they are convenient for scaling up production due to the possibility of low-cost melt processing [196]. Polycarbonate has also been reported to have biodegradability [197–199].

The conductive ink had both carbon black and graphene nanoplatelet as functional materials. Carbon black and graphene nanoplatelet were combined with two goals in mind. First, this combination could make the functional materials more dispersible due to the implementation of carbon black while having the high conductivity and good mechanical properties of graphene. Second, carbon black could act as a filler between the graphene nanoplatelet, enhancing the conductive pathway and resulting in higher conductivity [191].

The positive impact of the composite on conductivity was evaluated by measuring the sheet resistance of inks prepared with changing amounts of carbon black and graphene. Figure 4.1 (a) shows that when the ink was composed of only graphene (40 mg/mL) as the conductive material, the average sheet resistance was 1125 Ω/sq. But with the ink with an additional 10 mg/ml of carbon black, an almost one-fourth decrease in the resistance (292 Ω/sq) was observed. Similarly, in ink with only 40 mg/ml of carbon black as the conductive material, the resistance was observed to be 5000 Ω/sq, which was expected because carbon black has a much lower electrical conductivity than graphene; however, when

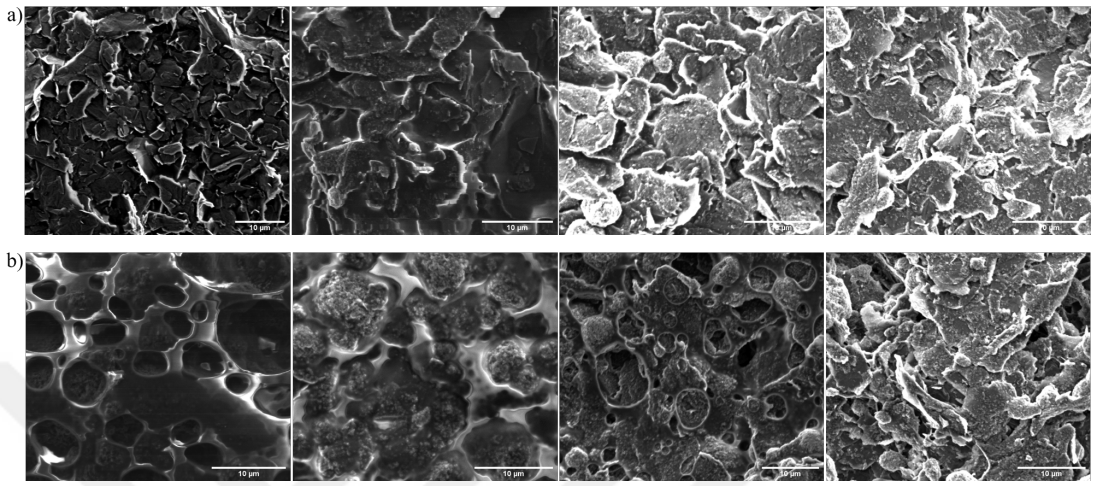

Figure 4.2: The SEM images of printed inks with increasing amounts of (a) carbon black (0 mg, 10 mg, 20 mg, and 30 mg, per ml, from left to right) and (b) graphene (0 mg, 10 mg, 20 mg, and 30 mg, per ml, from left to right).

another ink was formulated with an additional 10 mg of graphene, the resistance decreased dramatically (762 Ω/sq) (Figure 4.1 (b)). This phenomenon could be related to the filler behavior of carbon black within the graphene distribution, which was activated carbon black, and graphene composites were introduced into the solutions. After adding further amounts of graphene and carbon black, linear decreases in resistance were observed in both cases. The lowest sheet resistance achieved was 135 Ω/sq, developed with 50 mg/ml polycarbonate binder, 40 mg/ml of carbon black, and 30 mg/ml of graphene nanoplatelet.

The SEM images further corroborate this explanation, showing a network of graphene sheets in ink without carbon black and with increasing amounts of added carbon black, a well-distributed carbon black particle filler within the graphene network (Figure 4.2).

On the other hand, in the printed ink that had only carbon black as the functional material, the SEM images revealed carbon black particles in the polycarbonate matrix without a well-established network, explaining the significantly higher resistance in comparison to other inks. However, the inclusion of graphene improved the network, decreasing the resistance as a result.

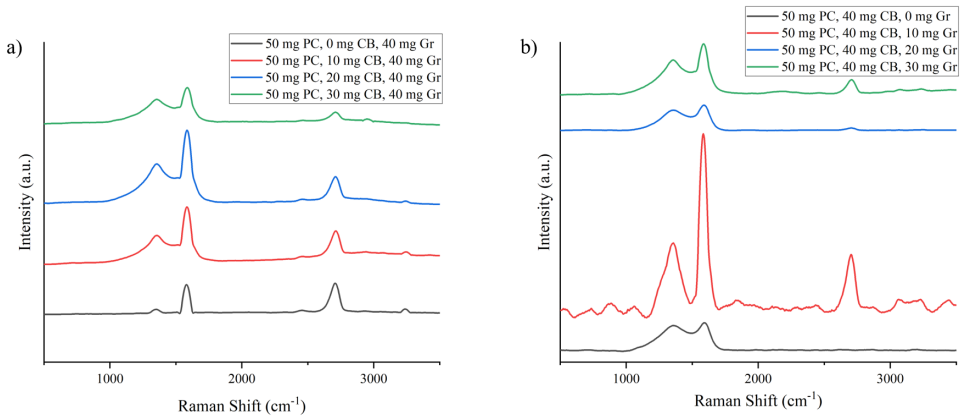

Figure 4.3: The Raman spectroscopy of printed inks with increasing amounts of (a) carbon black (0 mg, 10 mg, 20 mg, and 30 mg, per ml, from left to right) and (b) graphene (0 mg, 10 mg, 20 mg, and 30 mg, per ml, from left to right).

The Raman spectroscopy showed the existence of both carbon black and graphene in the complex. In Figure 4.3 (a), the printed ink with only graphene exhibited a G peak (at approximately 1580 cm^{-1}) denoting graphitic that could be associated with graphitized carbon structure, a 2D peak (at approximately 2720 cm^{-1}) denoting a higher order of D peaks without any disorder or defects, and barely any D peak (at approximately 1350 cm^{-1}) denoting defects in the carbon material lattice structure, which could be identified as the characteristics of graphene [200–203]. With the addition of carbon black, we could observe a more noticeable presence of D peaks [204]. On the other hand, the absence of 2D peaks for the ink that only had carbon black could be correlated with the absence of graphene in the ink, and this was further endorsed by the presence of 2D peaks after the addition of graphene in the ink (Figure 4.3 (b)) [200–203].

XPS analysis was done on all the samples with both changing amounts of carbon black (Figure 4.4) and graphene (Figure 4.5). In both cases, the deconvolution of C1s spectra showed three component peaks, which could be attributed to carbon with sp2 hybridization (C=C) at 284 eV, carbon with sp3 hybridization (C–C) at 286 eV, and the carbonyl carbon (C=O) at 290 eV. The O1s peak could be deconvoluted into a (C–C) peak at 532 eV and a (C=O) peak at 534 eV. All these functional groups should be present in pristine carbon materials [205–207].

DCM was used as the solvent for the inks; however, DCM is a toxic material [208]. The Cl2p spectra proved that there was no chlorine (Cl)-based element present in the printed ink, which means that DCM was evaporated in all cases (Figure 4.4 and Figure 4.5).

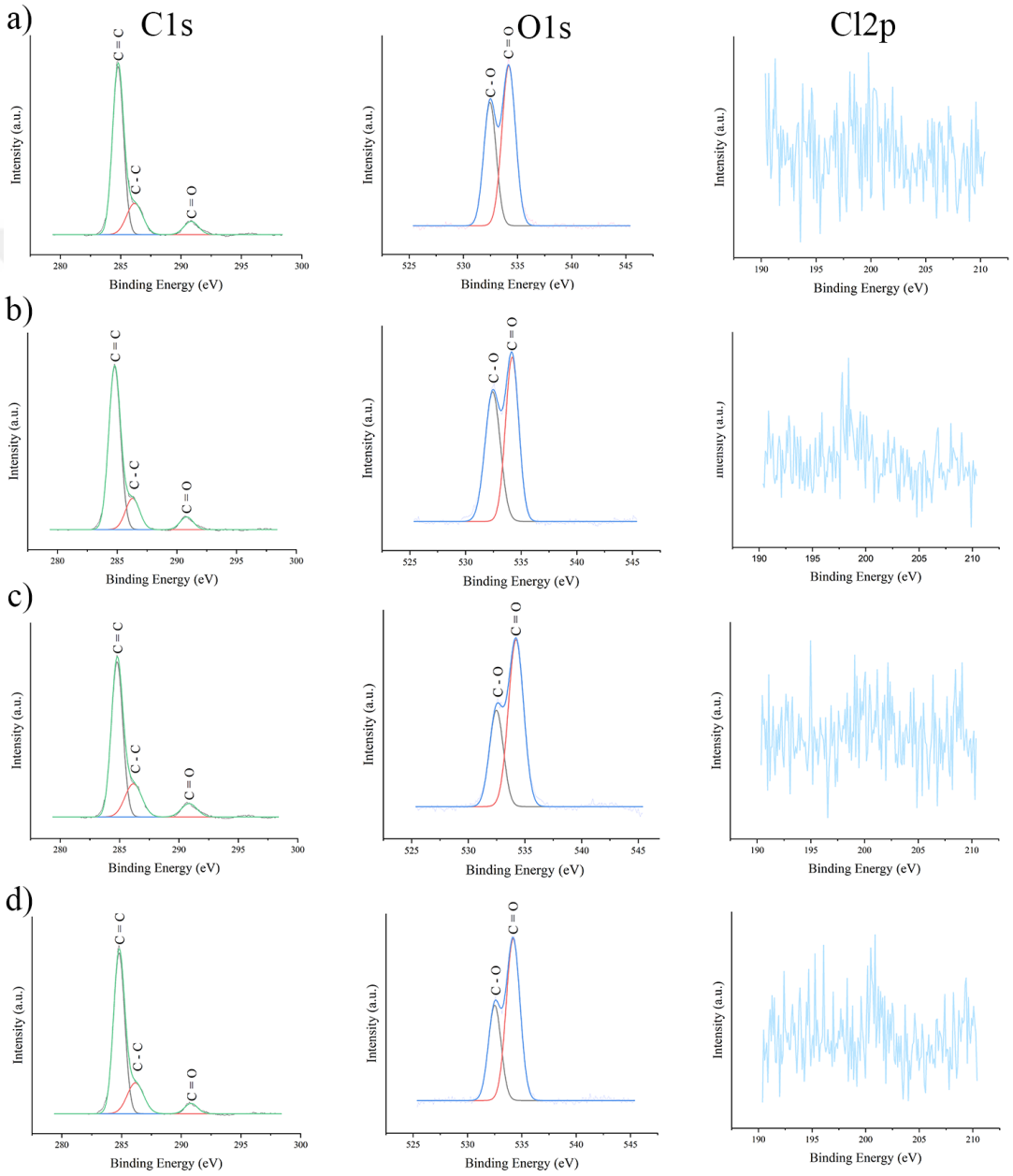

Figure 4.4: The XPS spectra of carbon black-graphene composite ink with (a) 0 mg, (b) 10 mg, (c) 20 mg, and (d) 30 mg, per ml of carbon black, and 40 mg per ml of graphene.

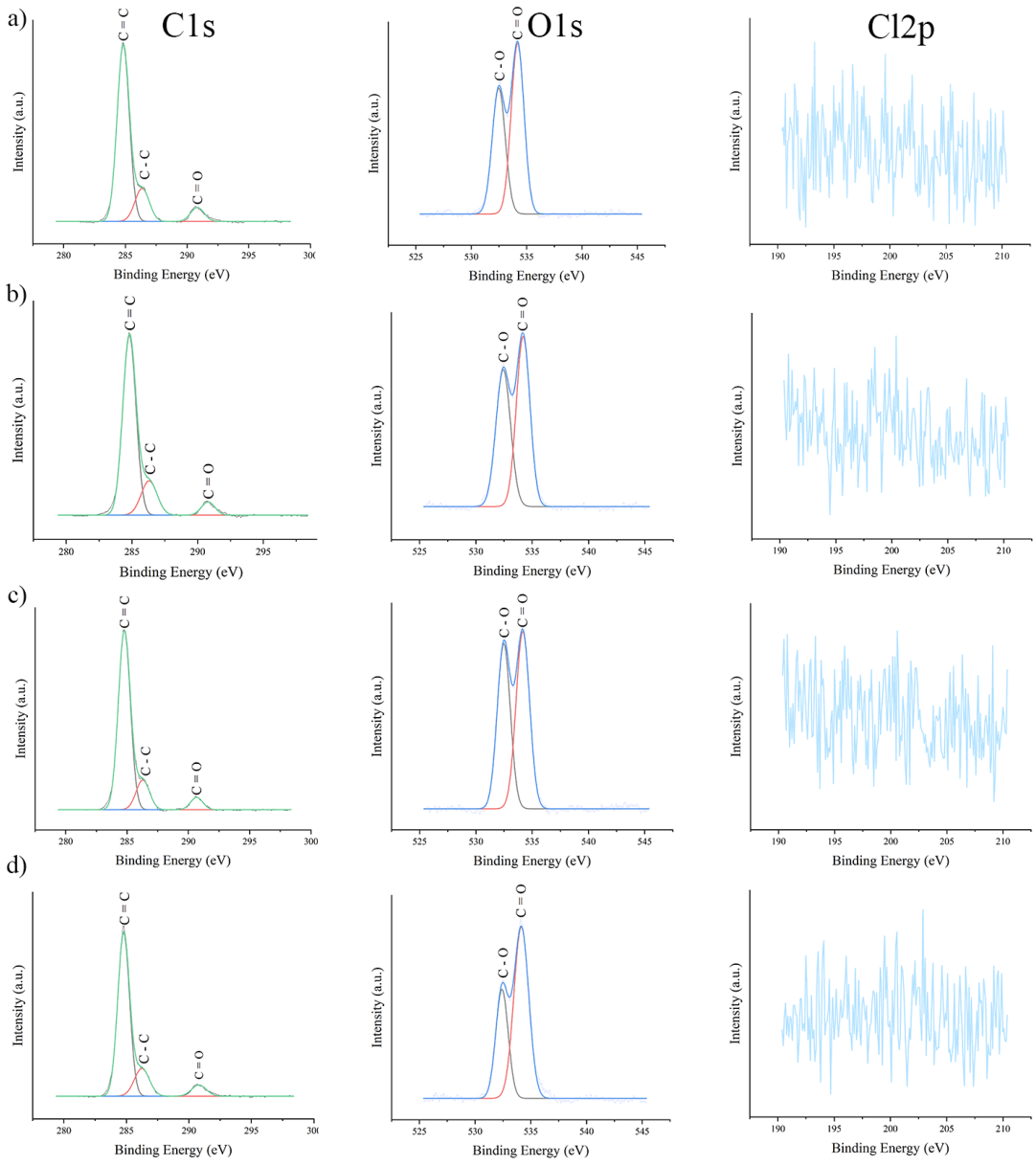

Figure 4.5: The XPS spectra of carbon black-graphene composite ink with (a) 0 mg, (b) 10 mg, (c) 20 mg, and (d) 30 mg, per ml of graphene nanoplatelet, and 40 mg per ml of carbon black.

To further determine the safety of wearable devices, cell growth and viability experiments were conducted. 3T3 cells were incubated with a control group (Figure 4.6), along with three different inks: 1) ink with only 40 mg of graphene (Figure 4.7), 2) ink with only 40 mg of carbon black (Figure 4.8), and 3) ink with both 40 mg of graphene and 40 mg of carbon black (Figure 4.9). After incubation, all experimental groups were marked with Hoechst 33342, Calcein AM, and Ethidium Homodimer-1 for visualization and both bright field and fluorescence images were obtained for all experimental groups for comparison. The bright field images are presented in Figures (4.6 (a), 4.7 (a), 4.8 (a), and 4.9 (a)); the blue cells represent 3T3 cells nuclei marked with Hoechst 33342; the green cells represent the live cells marked with calcein-AM in Figures (4.6 (c), 4.7 (c), 4.8 (c), and 4.9 (c)); the red cells represent the dead cells marked with ethidium homodimer-1in Figures (4.6 (d), 4.7 (d), 4.8 (d), and 4.9 (d)); and finally, the Figures (4.6 (e), 4.7 (e), 4.8 (e), and 4.9 (e)) shows merged images of all stainings.

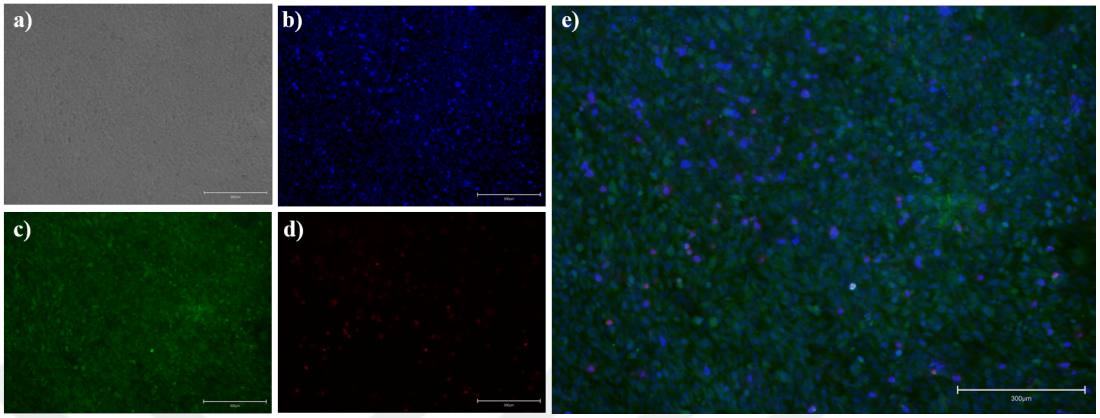

Figure 4.6: Microscope images of control 3T3 cells for 7 days; (a) Light microscope image at day 7, (b) Image of 3T3 cells marked with Hoechst 33342, (c) Image of live 3T3 cells marked with Calcein-AM, (d) Image of dead 3T3 cells marked with Ethidium homodimer-I, and (e) Merged image of all staining.

The viability of 3T3 cells incubated with the samples printed with inks that had only 40 mg/ml of graphene, only 40 mg/ml of carbon black, and both 40 mg/ml of graphene and carbon black were found to be 88%, 90.7%, and 82.2%, respectively (Figure 4.10), which means all of them were found to be non-cytotoxic [209].

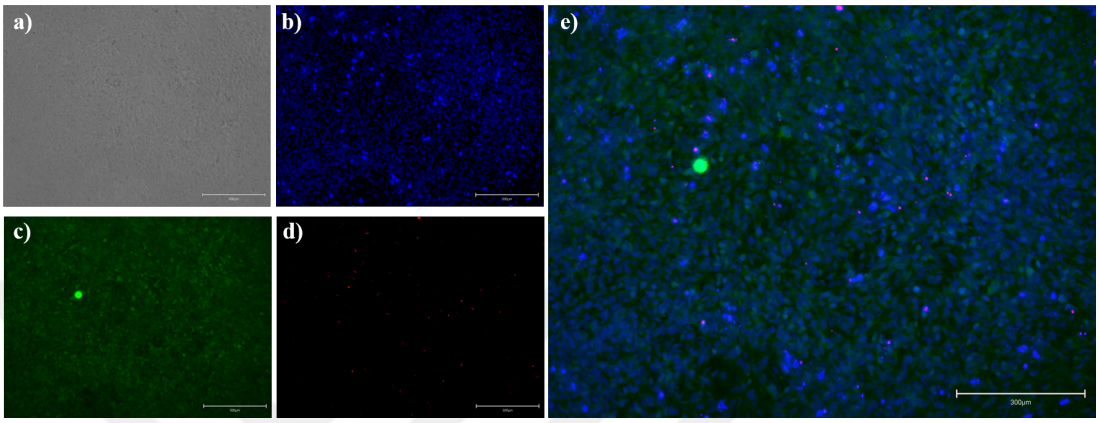

Figure 4.7: Microscope images of 3T3 cells incubated with samples printed with the ink composed of 40 mg of graphene for 7 days; (a) Light microscope image at day 7, (b) Image of 3T3 cells marked with Hoechst 33342, (c) Image of live 3T3 cells marked with Calcein-AM, (d) Image of dead 3T3 cells marked with Ethidium homodimer-III, and (e) Merged image of all staining.

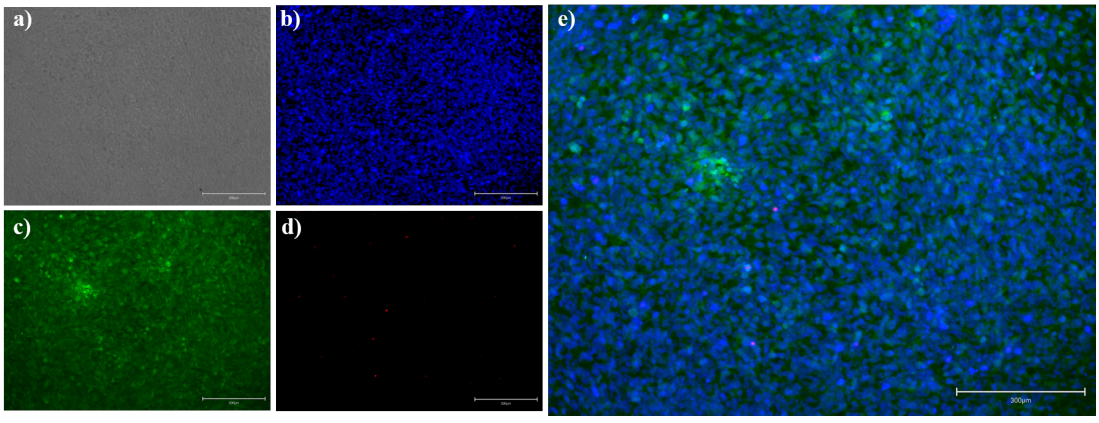

Figure 4.8: Microscope images of 3T3 cells incubated with samples printed with the ink composed of 40 mg of carbon black for 7 days; (a) Light microscope image at day 7, (b) Image of 3T3 cells marked with Hoechst 33342, (c) Image of live 3T3 cells marked with Calcein-AM, (d) Image of dead 3T3 cells marked with Ethidium homodimer-III, and (e) Merged image of all staining.

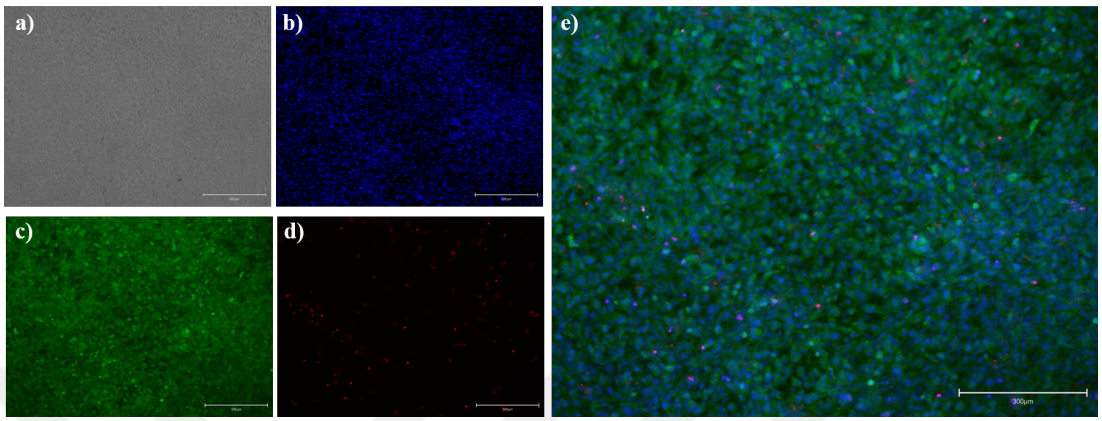

Figure 4.9: Microscope images of 3T3 cells incubated with samples printed with the ink composed of both 40 mg of graphene and carbon black for 7 days; (a) Light microscope image at day 7, (b) Image of 3T3 cells marked with Hoechst 33342, (c) Image of live 3T3 cells marked with Calcein-AM, (d) Image of dead 3T3 cells marked with Ethidium homodimer-III, and (e) Merged image of all staining.

Flow cytometry was also performed to assess the viability of 3T3 cells incubated with only 40 mg/ml of graphene, only 40 mg/ml of carbon black, and both 40 mg/ml of graphene and carbon black for 7 days (Figure 4.11). The results were found to be 92.7% for the sample with only 40 mg/ml of graphene ink, 89.5% for the sample with only 40 mg/ml of carbon black, and 85.0% for the sample with both 40 mg of graphene and carbon black ink.

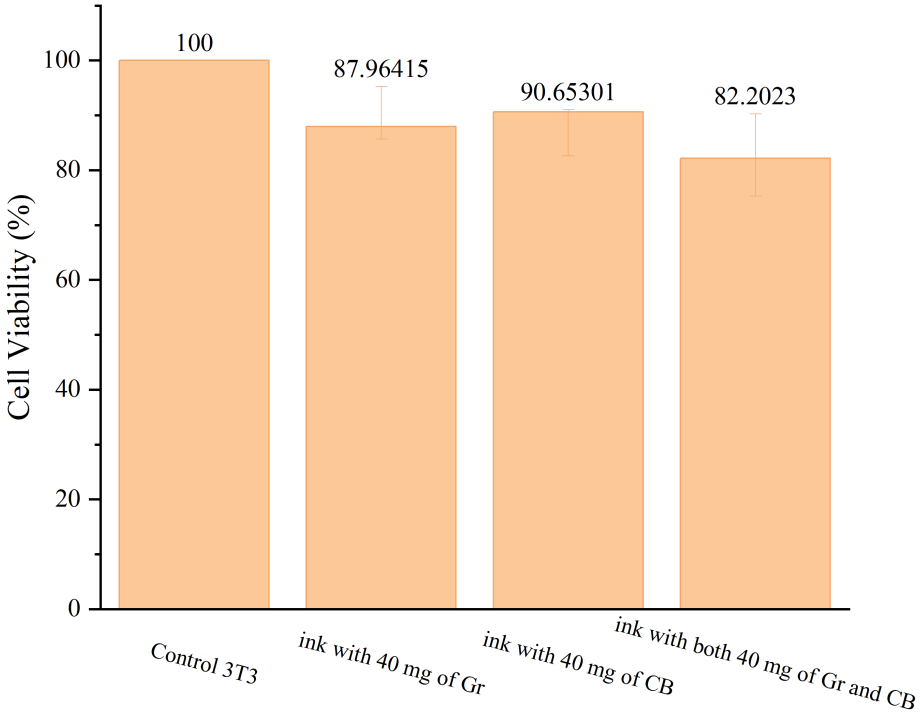

Figure 4.10: The cell viability (percentage) of samples printed with inks that had only 40 mg/ml of graphene, only 40 mg/ml of carbon black, and both 40 mg/ml of graphene and carbon black.

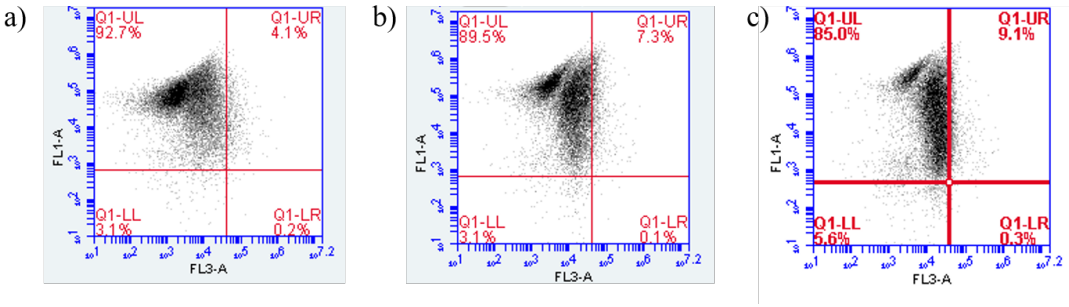

Figure 4.11: The flow cytometry results of samples printed with inks that had (a) only 40 mg/ml of graphene, (b) only 40 mg/ml of carbon black, and (c) both 40 mg/ml of graphene and carbon black.

4.2 Performance Test of Capacitive Touch Sensor

The performance of the interdigitated capacitive touch sensor was evaluated using time and pressure as variables. For the first experiment, three different amounts of pressure (5 kPa, 30 kPa, 45 kPa) were applied to the sensor at a fixed time (5 sec) (Figure 4.12). The initial capacitance of the sensor has been approximately 3.6 pF for all cases. The sensor exhibited an average capacitance of around 158.5 pF for 5 kPa pressure, 251.6 pF for 30 kPa, and 384.3 pF for 5 kPa, 30 kPa, and 45 kPa, respectively, along with consistent and repeatable performance.

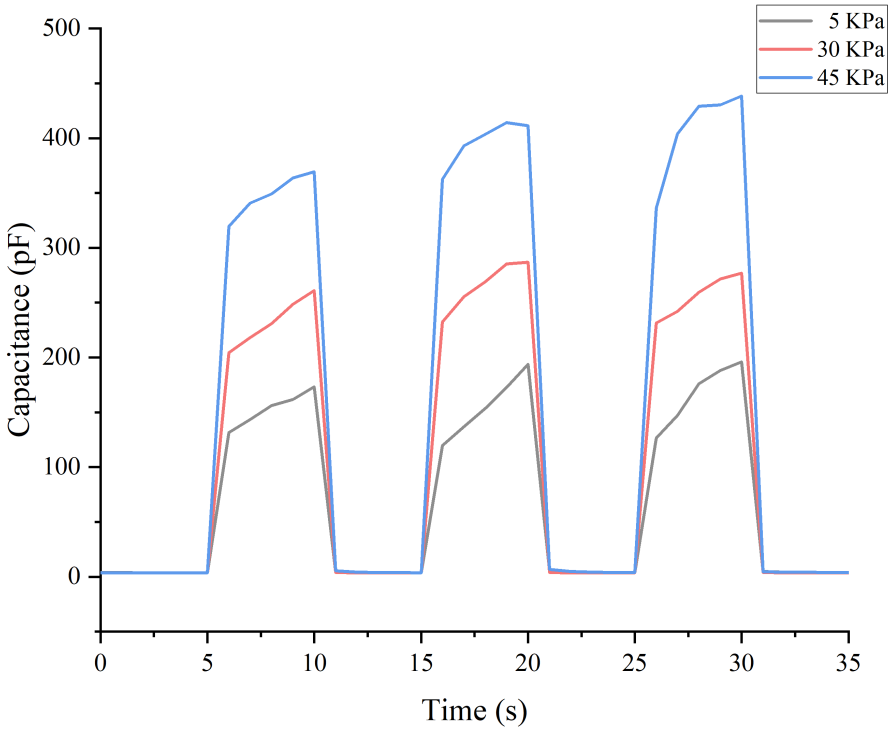

Figure 4.12: The performance of the capacitive sensor for a fixed time (5 sec) at three different pressure loads (5 kPa, 30 kPa, 45 kPa).

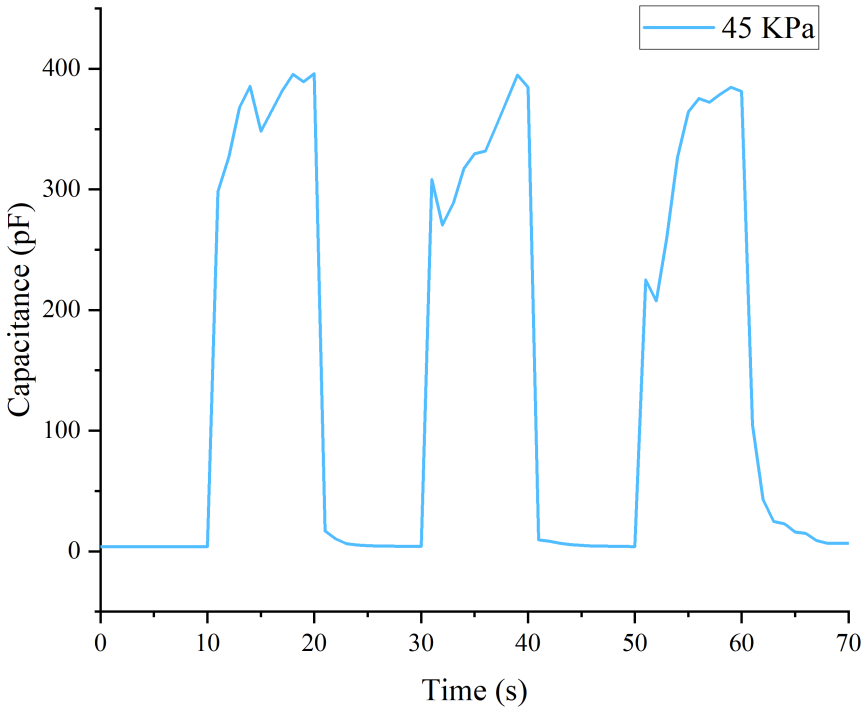

Figure 4.13: The performance of the capacitive touch sensor for a fixed time (10 sec) at 45 kPa pressure load.

The sensor performance and stability for a longer time (10 sec) were also evaluated (Figure 4.13). The sensor exhibited a similar level of capacitance change for 45 kPa pressure for both 5 and 10 seconds with consistent repeatability. The highest capacitance for the 10-second period measurements was around 396.04 pF.

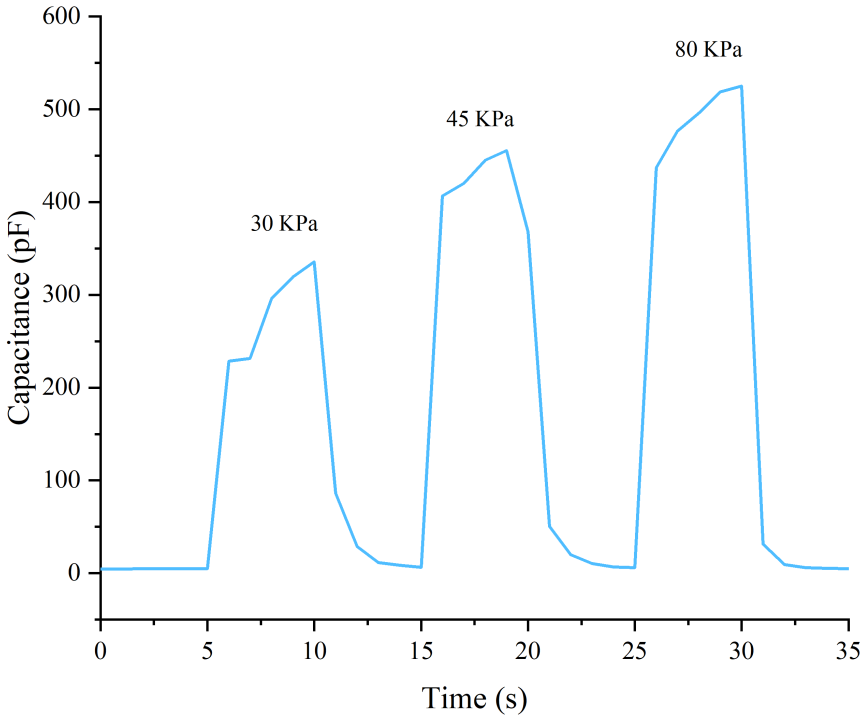

Figure 4.14: The performance of capacitive touch sensor with varying pressure (30 kPa, 45 kPa, and 80 kPa) loading and unloading cycles.

Furthermore, the sensor was also able to detect dynamic pressure (30 kPa, 45 kPa, 80 kPa) loading and unloading cycles (Figure 4.14). The average capacitance for 30 kPa, 45 kPa, and 80 kPa were 282.2 pF, 419 pF, and 490.6 pF, respectively.

Furthermore, the response time of the touch sensor has been exhibited using the charging and discharging cycle time of the capacitive sensor in Figure 4.15. The sensor could measure the pressure of 160 pF generated through touch in 240 milliseconds. After 5 seconds of settling down time, the capacitance was 287 pF, and when the pressure was removed, the sensor capacitance was at 87 pF at 240 milliseconds, and it could recover its original capacitance from 287 pF in 700 milliseconds.

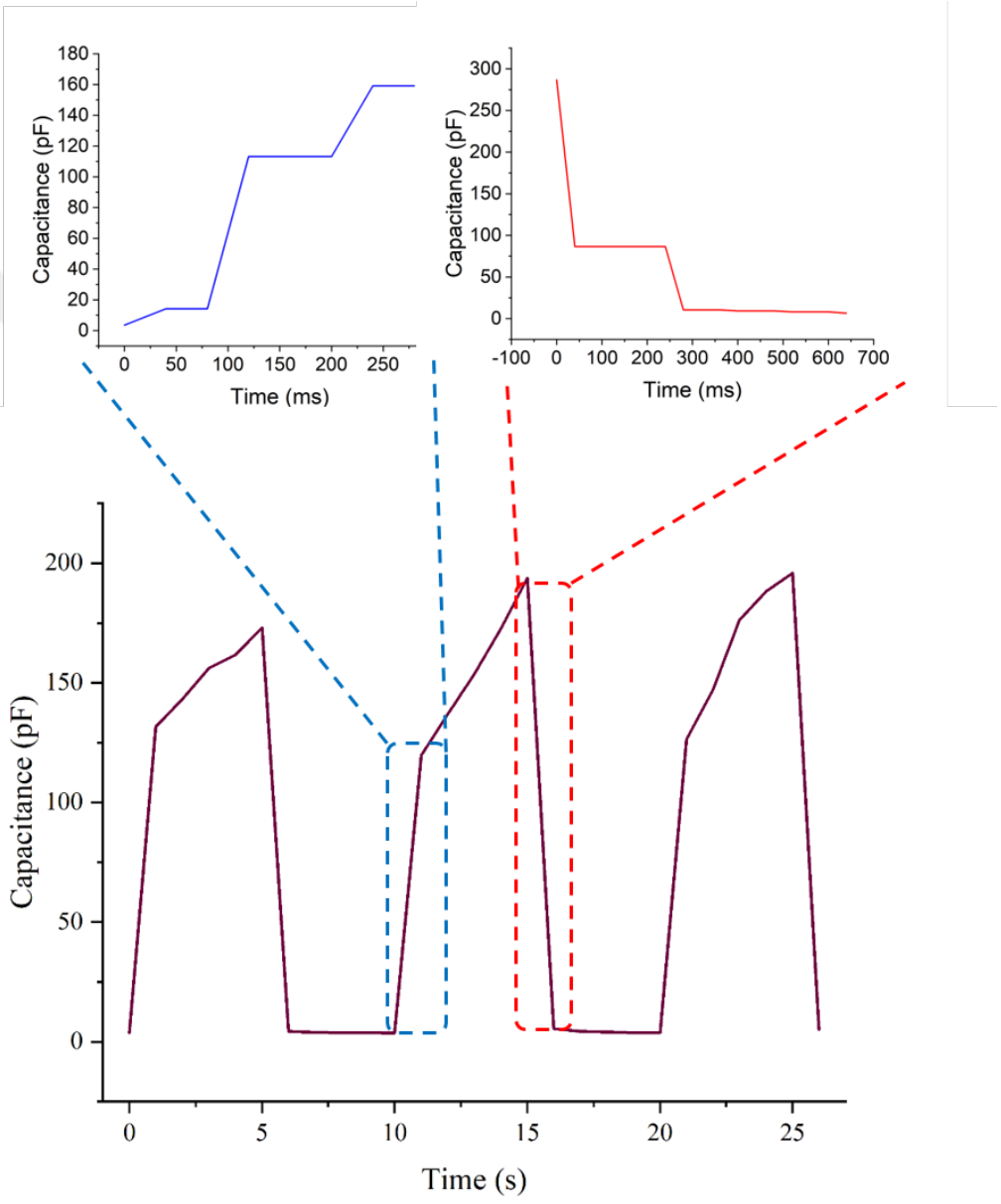

Figure 4.15: The response time of the capacitive touch sensor.

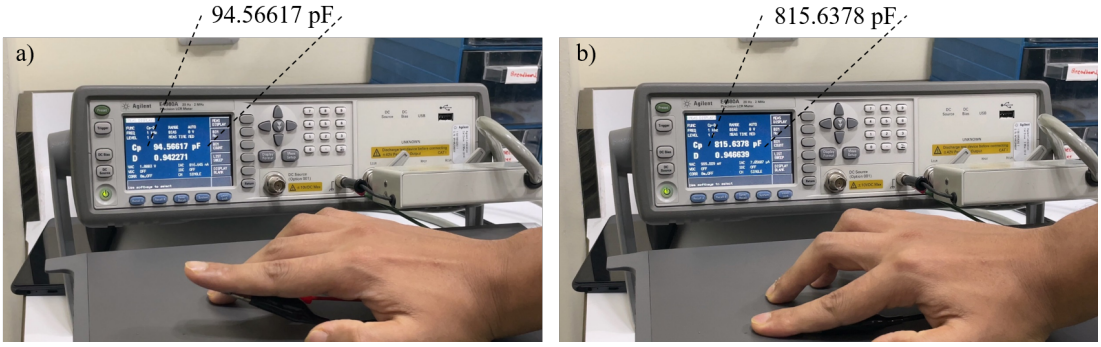

Figure 4.16: The capacitance measurement of the tattoo sensor on a fingertip when (a) not in contact with the surface and (b) in contact with the surface.

Figure 4.16 (a) shows the initial capacitance (94.56617 pF) of the tattoo sensor without contact with any surface, and Figure 4.16 (b) shows the change in capacitance (815.6378 pF) when the sensor comes in contact with the surface.

4.3 Performance Test of Resistive Strain Sensor

The performance of the textile-based strain sensor, with a dimension of 1 cm x 3 cm, was evaluated using time and angle as variables. The initial average resistance was found to be around 55 k Ω. For the first experience, the resistance was measured after bending the sensor at three different angles (30°, 60°, and 90°) for 5 seconds (Figure 4.17). The average resistance for 30°, 60°, and 90° angle bending was found to be 17.6 k Ω , 10.2 k Ω, and 4.3 k Ω.

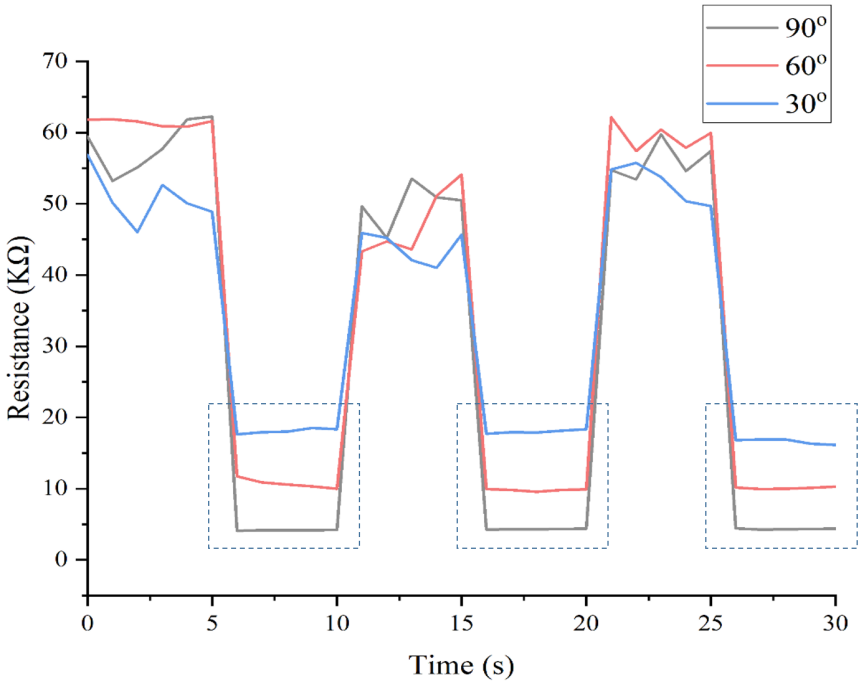

Figure 4.17: The performance of the resistive strain sensor for a fixed time (5 sec) at three different angles (30°, 60°, and 90°).

The strain sensor's performance with 90° bending for a shorter (5 sec) and longer (10 sec) motion time was evaluated to see if the sensor was capable of detecting fast and slow motion (Figure 4.18). The change in resistance was slower with slower motion but with a similar trend. The initial resistance was 43 k Ω, which dropped to 15 k Ω, then 10.2 k Ω, and after that 5.1 k Ω at 30°, 60°, and 90° with an overall motion time of 5 seconds. With the overall motion time of 10 seconds, the resistance dropped to 17 k Ω, then 13.8 k Ω, and finally to 6.5 k Ω

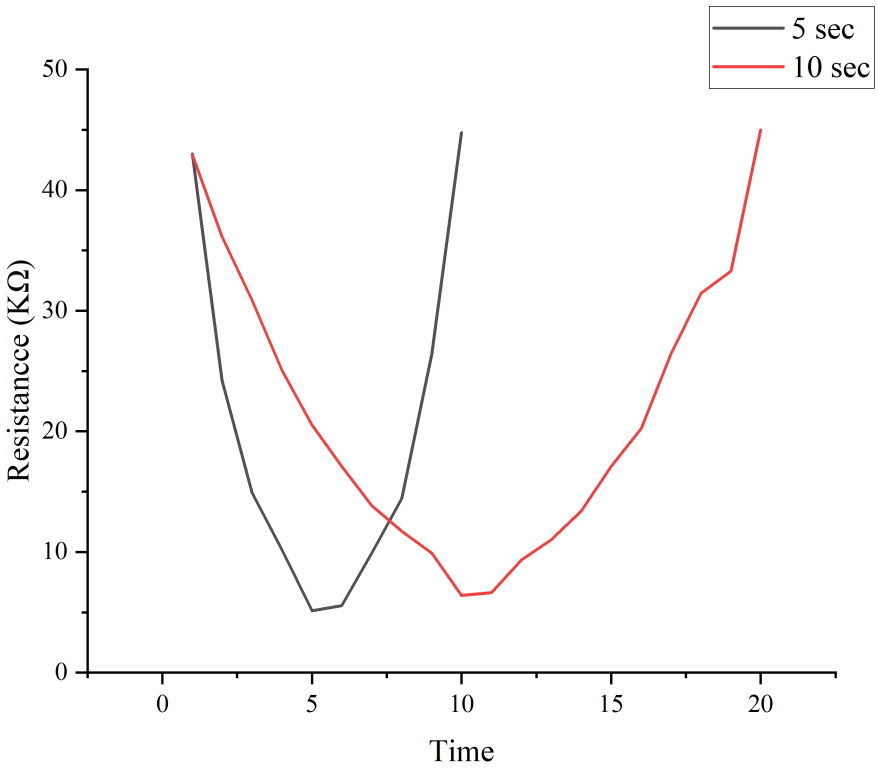

Figure 4.18: The performance of the resistive strain sensor for different motion times (5 and 10 sec).

at 30°, 60°, and 90°, respectively, from the initial resistance of 43 k Ω, but at a slower pace.

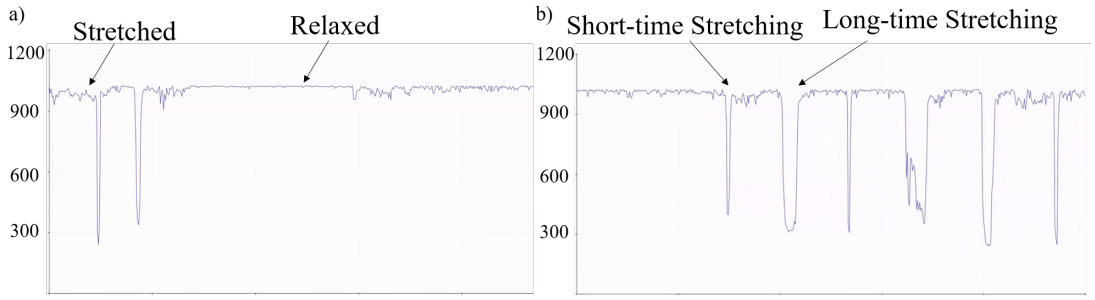

Figure 4.19: The change in voltage in a voltage divider circuit due to (a) stretching and relaxing and (b) short- and long-time stretching of the textile strain sensor.

A voltage divider circuit with an arduino setup was prepared and used to measure the voltage change by stretching and relaxing the textile strain sensor real-time. The stable voltage during the relaxed state of the fabric and the voltage drop during stretching were exhibited in Figure 4.19 (a). Furthermore, faster stretching and relaxing in a short time could be differentiated from stretching of the strain sensor for a longer time based on the consistent and distinguished voltage change trend between them (Figure 4.19 (b)).

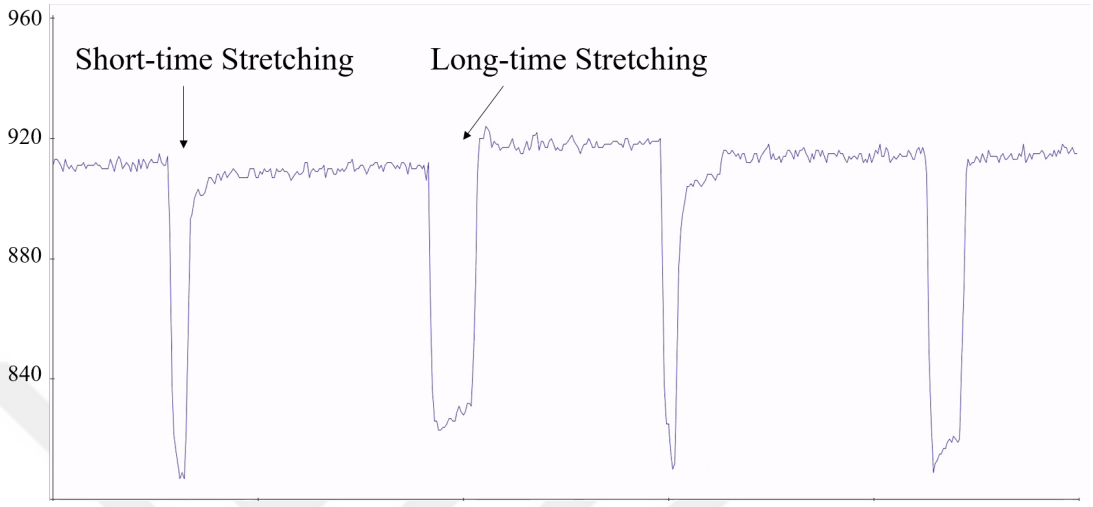

Figure 4.20: The performance of the textile strain sensor after 10 washing cycles.

A major requirement of any textile-based sensor would be washability. Moreover, the fabric sensor must be resistant to the alkaline characteristic (pH10) of standard detergent solutions[210]. Therefore, to evaluate the durability of the textile strain sensor, it was subjected to 10 washing cycles (10 minutes per cycle) with commercially available liquid detergent and high-speed rotation to emulate the centrifugal force, friction force, and water pressure inside commercially available standard washing machines [211]. After these 10 washing cycles, the sensor was dried at room temperature and again tested with the same voltage divider arduino setup previously mentioned. And, it was possible to generate a similar performance trend with the strain sensor even after the 10 cycles of washing (Figure 4.20).

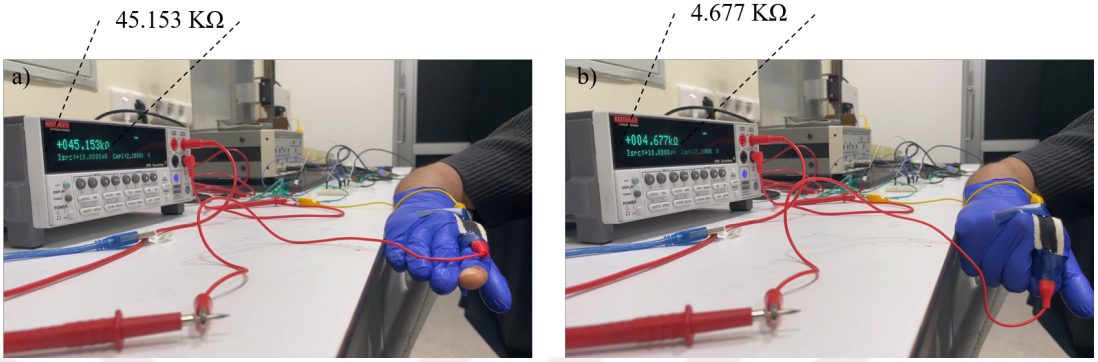

Figure 4.21: The resistance measurement of the fabric sensor (a) without any bending when the fist is open, and (b) with 90° bending with the fist closed.

In Figure 4.21 (a), the initial resistance of the fabric sensor without any bending was measured at 45.153 k Ω, and Figure 4.21 (b) shows the decrease of the resistance to 4.677 k Ω when the sensor was bent due to the first closing.

Chapter 5

Conclusion and Outlook

In this work, a methodology for formulating novel conductive ink was formulated to be utilized in developing wearable technology, which are biocompatible. Furthermore, the potential of conductive ink in flexible wearable technology was demonstrated by fabricating a tattoo-based capacitive touch sensor and a textile-based flexible strain sensor by using a simple stencil printing-inspired methodology. The developed sensor was cost-effective to produce; with approximately one US dollar, it was possible to produce 18-20 touch sensing tattoos, and with the same cost (about US$1), 8-10 fabric-based strain sensors were possible to produce.

In the first phase of this study, a simple and easy-to-produce conductive ink was developed. Polycarbonate – a thermoplastic polymer - was selected as the binder for the conductive ink, due to its cost-effectiveness, wide availability, good mechanical properties, adhesiveness, and easy processibility. A combination of graphene nanoplatelet and carbon black was used as the functional materials to take advantage of the synergistic effects of this composite due to their structures, which helped with creating an efficient conductive network due to carbon black acting as a filler between graphene sheets and improving the electrical performance. Furthermore, the presence of carbon black also helped with better dispersion of graphene, which has a tendency of restacking.

Through sheet resistance measurements, it was observed that introducing a second conductive material, instead of using only carbon black or graphene, resulted in a significant decrease in resistance value. The ink composed of only 40 mg/ml of graphene nanoplatelet exhibited a sheet resistance of 1125 Ω/sq on average. However, introducing only 10 mg/ml of carbon black into the ink, while keeping the amount of graphene nanoplatelet fixed to 40 mg/ml of graphene resulted in sheet resistance of 292 Ω/sq, which is almost one-fourth of the sheet resistance of the ink with only 40 mg/ml of graphene. Similarly, when the sheet resistance of the ink with only 40 mg/ml carbon black was measured, it was found to be 5000 Ω/sq. The higher resistance value of the carbon black ink was expected because carbon black intrinsically has a much higher resistance than graphene, so formulating two different inks with graphene and carbon black using the same ratio should result in higher resistance in the carbon black ink. However, with the addition of 10 mg/ml of graphene nanoplatelet with 40 mg/ml of carbon black, the sheet resistance dropped to 762 Ω/sq, which is an 85% decrease in sheet resistance that was observed in the conductive ink prepared with 40 mg/ml of carbon black only. The scanning electron microscope further endorsed the concept of carbon black particles acting as filler materials among graphene nanoplatelet sheets. Raman spectroscopy was used to prove the existence of both graphene and carbon black in the complex material, which showed the generation of distinctive peaks with the addition of new carbon materials into the system. Generation of a 2D peak (at approximately 2720 cm-1) denoting a higher order of D peaks without any disorder or defects specific to graphene was observed to be generated with the addition of graphene that did not exist for the ink formulated with only carbon black. Similarly, with the addition of carbon black, we could observe a more noticeable presence of a D peak, denoting defects in the carbon material lattice structure. Dichloromethane was used as the solvent to prepare the inks because of its performance as a dispersant, its capability of dissolving polycarbonate to prepare a homogenous binder solution, and also its fast evaporation rate that could help with faster sensor fabrication. However, dichloromethane is a toxic chemical that is harmful when it comes in contact with human skin. The X-ray photoelectron Spectroscopy exhibited no existence of chlorine in the printed inks, proving that the printed inks do not hold

any amount of dichloromethane, making it safe for wearable applications. This claim was further corroborated by cell viability tests that showed that the printed sensor electrodes were fully biocompatible with always a cell viability percentage of above 80%.

The lowest sheet resistance achieved after experimenting with different quantities of graphene and carbon black was 135 Ω/sq, developed with 50 mg/ml polycarbonate binder, 40 mg of carbon black, and 30 mg of graphene nanoplatelet, and this ink was used to develop the capacitive touch sensor and resistive strain sensor.

For the fabrication of both sensors, a stencil-printing methodology was utilized due to its simplicity and cost-effectiveness. The stencils were produced from double-sided adhesives, and the desired patterns were developed on the stencil using a CO_2 laser-based cutting and engraving equipment. After that, the stencils were attached to the substrates (commercial tattoo paper for the capacitive touch sensor and chemically untreated cotton fabric for the resistive strain sensor), and carbon material-based conductive ink was printed and dried at room temperature before removing the stencils to acquire the desired pattern on the substrates. The stencils could be produced with multiple patterns to produce a large number of sensors simultaneously, which showed high potential to be useful in mass scale-up of production for such stencil-printed sensors. Furthermore, stencil printing is already a well-established and widely used methodology, especially in textile industries. Therefore, no additional complicated step is needed to be introduced when considering mass manufacturing in textile industries.

In the second phase of the work, a tattoo-based capacitive touch sensor was developed that was capable of differentiating between three different levels of pressure loads. The tattoo sensor was capable of exhibiting consistent and reproducible performance at different time ranges and dynamic pressure loads as well. The different pressure loads tested for the sensor were 5 kPa, 30 kPa, and 45 kPa, and the sensor exhibited an average capacitance of around 158.5 pF, 251.6 pF, and 384.3 pF, 342 pF, respectively, for these pressure loads, increasing from an initial capacitance of around 3.6 pF. The performance of the capacitive sensor

for a longer time at a fixed rate of pressure was also evaluated, and consistent performance was observed with multiple repetitions. Furthermore, the sensor was able to demonstrate a fast detection of touch and showed a change in capacitance in 240 milliseconds.

In the third phase of this thesis, the developed conductive ink was used on commercially available cotton fabric to fabricate a stretchable strain sensor capable of monitoring human motion utilizing the resistance change of the fabric due to structural deformation resulting in a change of conductive pathway. The initial resistance of the 1 x 3 cm fabric was found to be, on average, 55 k Ω. And, with three bending angles (30°, 60°, and 90°), the resistance dropped to approximately 17.6 k Ω, 10.2 k Ω, and 4.3 k Ω, respectively, which could be utilized in differentiating between different levels of bending in human joints. The sensor was also capable of consistently differentiating between fast stretching-relaxing cycles and slow stretching-relaxing cycles. Furthermore, the textile strain sensor was capable of exhibiting a similar performance trend even after 10 cycles of washing.

The future steps of this work would be to further improve the performance of the sensors by utilizing different substrates, structural designs, and fabrication methods. Commercially available tattoo paper was used for printing the tattoo-based capacitive touch sensor. Investigating different flexible polymers with high dielectric constants as substrates to develop the tattoo should further improve the capacitive performance of the touch sensor. For the textile-based strain sensor, functionalizing textile yarns and developing the fabric bottom-up should provide much more control over the structure and design of the sensor, resulting in improved performance. Moreover, it should ease up the path of commercial development of functional textiles even more without introducing additional complex steps in the mass production methodology.

Chapter 6

Bibliography

[1] P. Wang, M. Hu, H. Wang, Z. Chen, Y. Feng, J. Wang, W. Ling, and Y. Huang, The Evolution of Flexible Electronics: From Nature, Beyond Nature, and To Nature, Advanced Science 7, 2001116 (2020).

[2] Y. Lee, J. Park, A. Choe, S. Cho, J. Kim, and H. Ko, Mimicking Human and Biological Skins for Multifunctional Skin Electronics, Advanced Functional Materials 30, 1904523 (2020).

[3] Q. Hua, J. Sun, H. Liu, R. Bao, R. Yu, J. Zhai, C. Pan, and Z. L. Wang, Skin-Inspired Highly Stretchable and Conformable Matrix Networks for Multifunctional Sensing, Nat Commun 9, 244 (2018).

[4] H. Ouyang et al., Self-Powered Pulse Sensor for Antidiastole of Cardiovascular Disease, Advanced Materials 29, 1703456 (2017).

[5] B. Meng, W. Tang, Z. Too, X. Zhang, M. Han, W. Liu, and H. Zhang, A Transparent Single-Friction-Surface Triboelectric Generator and Self-Powered Touch Sensor, Energy Environmental Science 6, 3235 (2013).

[6] Y. Kim et al., A Bioinspired Flexible Organic Artificial Afferent Nerve, Science 360, 998 (2018).

[7] S. Gupta, W. T. Navaraj, L. Lorenzelli, and R. Dahiya, Ultra-Thin Chips for High-Performance Flexible Electronics, Npj Flex Electron 2, 1 (2018). [8] Y. Z. N. Htwe and M. Mariatti, Printed Graphene and Hybrid Conductive Inks for Flexible, Stretchable, and Wearable Electronics: Progress, Opportunities, and Challenges, Journal of Science: Advanced Materials and Devices 7, 100435 (2022).

[9] D. Baran, D. Corzo, and G. T. Blazquez, Flexible Electronics: Status, Challenges and Opportunities, Front.Electron. 1, (2020).

[10] I. You, M. Kong, and U. Jeong, Block Copolymer Elastomers for Stretchable Electronics, Acc. Chem. Res. 52, 63 (2019).

[11] K. Sim, Z. Rao, F. Ershad, and C. Yu, Rubbery Electronics Fully Made of Stretchable Elastomeric Electronic Materials, Advanced Materials 32, 1902417 (2020).

[12] F. De Rossi, G. Renno, B. Taheri, N. Yaghoobi Nia, V. Ilieva, A. Fin, A. Di Carlo, M. Bonomo, C. Barolo, and F. Brunetti, Modified P3HT Materials as Hole Transport Layers for Flexible Perovskite Solar Cells, Journal of Power Sources 494, 229735 (2021).

[13] L. Li, L. Han, H. Hu, and R. Zhang, A Review on Polymers and Their Composites for Flexible Electronics, Materials Advances 4, 726 (2023).

[14] W. Kong, Y. Yang, Y. Wang, H. Cheng, P. Yan, L. Huang, J. Ning, F. Zeng, X. Cai, and M. Wang, An Ultra-Low Hysteresis, Self-Healing and Stretchable Conductor Based on Dynamic Disulfide Covalent Adaptable Networks, J. Mater. Chem. A 10, 2012 (2022).

[15] S. Li, Y. Cong, and J. Fu, Tissue Adhesive Hydrogel Bioelectronics, J. Mater. Chem. B 9, 4423 (2021).

[16] H. Liu et al., Electrically Conductive Polymer Composites for Smart Flexible Strain Sensors: A Critical Review, J. Mater. Chem. C 6, 12121 (2018).

[17] F.-R. Fan, Z.-Q. Tian, and Z. Lin Wang, Flexible Triboelectric Generator, Nano Energy 1, 328 (2012).

[18] H. Gao, J. Li, F. Zhang, Y. Liu, and J. Leng, The Research Status and Challenges of Shape Memory Polymer-Based Flexible Electronics, Materials Horizons 6, 931 (2019).

[19] D.-H. Kim, J. Xiao, J. Song, Y. Huang, and J. A. Rogers, Stretchable, Curvilinear Electronics Based on Inorganic Materials, Advanced Materials 22, 2108 (2010).

[20] C. F. Guo, T. Sun, Q. Liu, Z. Suo, and Z. Ren, Highly Stretchable and Transparent Nanomesh Electrodes Made by Grain Boundary Lithography, Nat Commun 5, 3121 (2014).

[21] M. Gong, L. Zhang, and P. Wan, Polymer Nanocomposite Meshes for Flexible Electronic Devices, Progress in Polymer Science 107, 101279 (2020).

[22] X. Xu et al., Thermally Stable, Highly Efficient, Ultraflexible Organic Photovoltaics, Proceedings of the National Academy of Sciences 115, 4589 (2018).

[23] I. You et al., Artificial Multimodal Receptors Based on Ion Relaxation Dynamics, Science 370, 961 (2020).

[24] H. He, L. Zhang, X. Guan, H. Cheng, X. Liu, S. Yu, J. Wei, and J. Ouyang, Biocompatible Conductive Polymers with High Conductivity and High Stretchability, ACS Appl. Mater. Interfaces 11, 26185 (2019).

[25] E. Zeglio, A. L. Rutz, T. E. Winkler, G. G. Malliaras, and A. Herland, Conjugated Polymers for Assessing and Controlling Biological Functions, Advanced Materials 31, 1806712 (2019).

[26] D. Melling, J. G. Martinez, and E. W. H. Jager, Conjugated Polymer Actuators and Devices: Progress and Opportunities, Advanced Materials 31, 1808210 (2019).

[27] Z. Zhang, M. Liao, H. Lou, Y. Hu, X. Sun, and H. Peng, Conjugated Polymers for Flexible Energy Harvesting and Storage, Advanced Materials 30, 1704261 (2018).

[28] J. Chen, J. Liu, T. Thundat, and H. Zeng, Polypyrrole-Doped Conductive Supramolecular Elastomer with Stretchability, Rapid Self-Healing, and Adhesive Property for Flexible Electronic Sensors, ACS Appl. Mater. Interfaces 11, 18720 (2019).

[29] Z. Wu, Y. Wang, X. Liu, C. Lv, Y. Li, D. Wei, and Z. Liu, Carbon-Nanomaterial-Based Flexible Batteries for Wearable Electronics, Advanced Materials 31, 1800716 (2019).

[30] C. M. Das, L. Kang, Q. Ouyang, and K.-T. Yong, Advanced Low-Dimensional Carbon Materials for Flexible Devices, InfoMat 2, 698 (2020).

[31] C. Wang, K. Xia, H. Wang, X. Liang, Z. Yin, and Y. Zhang, Advanced Carbon for Flexible and Wearable Electronics, Advanced Materials 31, 1801072 (2019).

[32] V. B. Mbayachi, E. Ndayiragije, T. Sammani, S. Taj, E. R. Mbuta, and A. ullah khan, Graphene Synthesis, Characterization and Its Applications: A Review, Results in Chemistry 3, 100163 (2021).

[33] D. Kireev, J. Kampfe, A. Hall, and D. Akinwande, Graphene Electronic Tattoos 2.0 with Enhanced Performance, Breathability and Robustness, Npj 2D Mater Appl 6, 1 (2022).

[34] E. A. Sousa, T. H. C. Lima, E. P. S. Arlindo, A. O. Sanches, W. K. Sakamoto, and G. de C. Fuzari-Junior, Multicomponent Polyurethane–Carbon Black Composite as Piezoresistive Sensor, Polym. Bull. 77, 3017 (2020).

[35] P. A. Ciullo and N. Hewitt, COMPOUNDING MATERIALS, in The Rubber Formulary, edited by P. A. Ciullo and N. Hewitt (William Andrew Publishing, Norwich, NY, 1999), pp. 4–49.

[36] A. Ji, Y. Chen, X. Wang, and C. Xu, Inkjet Printed Flexible Electronics on Paper Substrate with Reduced Graphene Oxide/Carbon Black Ink, J Mater Sci: Mater Electron 29, 13032 (2018).

[37] S. Yong, M. Liu, A. Komolafe, J. Tudor, and K. Yang, Development of a Screen-Printable Carbon Paste to Achieve Washable Conductive Textiles, Textiles 1, 3 (2021).

[38] J. R. Camargo et al., Development of Conductive Inks for Electrochemical Sensors and Biosensors, Microchemical Journal 164, 105998 (2021).

[39] V. K. Rao R, V. Abhinav K, K. P. S, and S. Prakash Singh, Conductive Silver Inks and Their Applications in Printed and Flexible Electronics, RSC Advances 5, 77760 (2015).

[40] W. Yang and C. Wang, Graphene and the Related Conductive Inks for Flexible Electronics, Journal of Materials Chemistry C 4, 7193 (2016).

[41] A. Khan, K. Rahman, S. Ali, S. Khan, B. Wang, and A. Bermak, Fabrication of Circuits by Multi-Nozzle Electrohydrodynamic Inkjet Printing for Soft Wearable Electronics, Journal of Materials Research 36, 3568 (2021).

[42] T.-K. Kang, Piezoresistive Characteristics of Nylon Thread Resistive Memories for Wearable Strain Sensors, Coatings 9, 10 (2019).

[43] A. M. Gaikwad, A. C. Arias, and D. A. Steingart, Recent Progress on Printed Flexible Batteries: Mechanical Challenges, Printing Technologies, and Future Prospects, Energy Technology 3, 305 (2015).

[44] W. Yang, Z. Hu, C. Zhang, Y. Guo, and J. Zhao, Screen Printing Preparation of High-Performance Flexible Planar Micro-Supercapacitors Based on MoS2 Nanoparticles Decorated Electrochemically Exfoliated Graphene, Electrochimica Acta 429, 141041 (2022).

[45] D. S. Saidina, N. Eawwiboonthanakit, M. Mariatti, S. Fontana, and

C. Hérold, Recent Development of Graphene-Based Ink and Other Conductive Material-Based Inks for Flexible Electronics, J. Electron. Mater. 48, 3428 (2019).

[46] S. K. Tam, K. Y. Fung, G. S. H. Poon, and K. M. Ng, Product Design: Metal Nanoparticle-Based Conductive Inkjet Inks, AIChE Journal 62, 2740 (2016).

[47] D. Kim and J. Moon, Highly Conductive Ink Jet Printed Films of Nanosilver Particles for Printable Electronics, Electrochem. Solid-State Lett. 8, J30 (2005).

[48] H. Wang, J. Fu, C. Wang, R. Zhang, Y. Yang, Y. Li, C. Li, Q. Sun, H. Li, and T. Zhai, A Universal Aqueous Conductive Binder for Flexible Electrodes, Advanced Functional Materials 31, 2102284 (2021).

[49] I. S. Yoon, Y. Oh, S. H. Kim, J. Choi, Y. Hwang, C. H. Park, and B.-K. Ju, 3D Printing of Self-Wiring Conductive Ink with High Stretchability and Stackability for Customized Wearable Devices, Advanced Materials Technologies 4, 1900363 (2019).

[50] B. Tian, W. Yao, P. Zeng, X. Li, H. Wang, L. Liu, Y. Feng, C. Luo, and W. Wu, All-Printed, Low-Cost, Tunable Sensing Range Strain Sensors Based on Ag Nanodendrite Conductive Inks for Wearable Electronics, Journal of Materials Chemistry C 7, 809 (2019).

[51] N. Ibrahim, J. O. Akindoyo, and M. Mariatti, Recent Development in Silver-Based Ink for Flexible Electronics, Journal of Science: Advanced Materials and Devices 7, 100395 (2022).

[52] D. Wang, Y. Zhang, X. Lu, Z. Ma, C. Xie, and Z. Zheng, Chemical Formation of Soft Metal Electrodes for Flexible and Wearable Electronics, Chem. Soc. Rev. 47, 4611 (2018).

[53] J. S. Kang, H. S. Kim, J. Ryu, H. Thomas Hahn, S. Jang, and J. W. Joung, Inkjet Printed Electronics Using Copper Nanoparticle Ink, J Mater Sci:

Mater Electron 21, 1213 (2010).

[54] Y. Kim, B. Lee, S. Yang, I. Byun, I. Jeong, and S. M. Cho, Use of Copper Ink for Fabricating Conductive Electrodes and RFID Antenna Tags by Screen Printing, Current Applied Physics 12, 473 (2012).

[55] T. S. Tran, N. K. Dutta, and N. R. Choudhury, Graphene Inks for Printed Flexible Electronics: Graphene Dispersions, Ink Formulations, Printing Techniques and Applications, Advances in Colloid and Interface Science 261, 41 (2018).

[56] Y. Yang, E. Noviana, M. P. Nguyen, B. J. Geiss, D. S. Dandy, and C. S. Henry, Paper-Based Microfluidic Devices: Emerging Themes and Applications, Anal. Chem. 89, 71 (2017).

[57] S. Bi, W. Dong, B. Lan, H. Zhao, L. Hou, L. Zhu, Y. Xu, and Y. Lu, Flexible Carbonic Pen Ink/Carbon Fiber Paper Composites for Multifunctional Switch-Type Sensors, Composites Part A: Applied Science and Manufacturing 124, 105452 (2019).

[58] L. A. Pradela-Filho, D. A. G. Araújo, R. M. Takeuchi, and A. L. Santos, Nail Polish and Carbon Powder: An Attractive Mixture to Prepare Paper-Based Electrodes, Electrochimica Acta 258, 786 (2017).

[59] Z. Chu, J. Peng, and W. Jin, Advanced Nanomaterial Inks for Screen-Printed Chemical Sensors, Sensors and Actuators B: Chemical 243, 919 (2017).

[60] Y. Gao, W. Shi, W. Wang, Y. Leng, and Y. Zhao, Inkjet Printing Patterns of Highly Conductive Pristine Graphene on Flexible Substrates, Ind. Eng. Chem. Res. 53, 16777 (2014).

[61] P. He, J. Cao, H. Ding, C. Liu, J. Neilson, Z. Li, I. A. Kinloch, and B. Derby, Screen-Printing of a Highly Conductive Graphene Ink for Flexible Printed Electronics, ACS Appl. Mater. Interfaces 11, 32225 (2019).

[62] Y. Sekertekin, I. Bozyel, and D. Gokcen, A Flexible and Low-Cost Tactile Sensor Produced by Screen Printing of Carbon Black/PVA Composite on Cellulose Paper, Sensors 20, 10 (2020).

[63] M. Santhiago, C. C. Corrêa, J. S. Bernardes, M. P. Pereira, L. J. M. Oliveira, M. Strauss, and C. C. B. Bufon, Flexible and Foldable Fully-Printed Carbon Black Conductive Nanostructures on Paper for High-Performance Electronic, Electrochemical, and Wearable Devices, ACS Appl. Mater. Interfaces 9, 24365 (2017).

[64] J. C. Yang, J. Mun, S. Y. Kwon, S. Park, Z. Bao, and S. Park, Electronic Skin: Recent Progress and Future Prospects for Skin-Attachable Devices for Health Monitoring, Robotics, and Prosthetics, Advanced Materials 31, 1904765 (2019).

[65] M. Wang, Y. Luo, T. Wang, C. Wan, L. Pan, S. Pan, K. He, A. Neo, and X. Chen, Artificial Skin Perception, Advanced Materials 33, 2003014 (2021).

[66] Z. Chen and Y. Wang, Ionic Skin: From Imitating Natural Skin to Beyond, Ind. Chem. Mater. 1, 224 (2023).

[67] K. Zhao, Y. Zhao, R. Qian, and C. Ye, Recent Progress on Tattoo-like Electronics: From Materials and Structural Designs to Versatile Applications, Chemical Engineering Journal 477, 147109 (2023).

[68] D.-H. Kim et al., Epidermal Electronics, Science 333, 838 (2011).

[69] H. Li et al., E-Tattoos: Toward Functional but Imperceptible Interfacing with Human Skin, Chem. Rev. 124, 3220 (2024).

[70] Y. Wang, Y. Qiu, S. K. Ameri, H. Jang, Z. Dai, Y. Huang, and N. Lu, Low-Cost, m-Thick, Tape-Free Electronic Tattoo Sensors with Minimized Motion and Sweat Artifacts, Npj Flex Electron 2, 1 (2018).

[71] J. R. Windmiller, A. J. Bandodkar, G. Valdés-Ramírez, S. Parkhomovsky,

A. G. Martinez, and J. Wang, Electrochemical Sensing Based on Printable Temporary Transfer Tattoos, Chem. Commun. 48, 6794 (2012).

[72] W. Jia, A. J. Bandodkar, G. Valdés-Ramírez, J. R. Windmiller, Z. Yang, J. Ramírez, G. Chan, and J. Wang, Electrochemical Tattoo Biosensors for Real-Time Noninvasive Lactate Monitoring in Human Perspiration, Anal. Chem. 85, 6553 (2013).

[73] A. J. Bandodkar, D. Molinnus, O. Mirza, T. Guinovart, J. R. Windmiller, G. Valdés-Ramírez, F. J. Andrade, M. J. Schöning, and J. Wang, Epidermal Tattoo Potentiometric Sodium Sensors with Wireless Signal Transduction for Continuous Non-Invasive Sweat Monitoring, Biosensors and Bioelectronics 54, 603 (2014).

[74] S. Kabiri Ameri, R. Ho, H. Jang, L. Tao, Y. Wang, L. Wang, D. M. Schnyer, D. Akinwande, and N. Lu, Graphene Electronic Tattoo Sensors, ACS Nano 11, 7634 (2017).

[75] D. Kireev, S. K. Ameri, A. Nederveld, J. Kampfe, H. Jang, N. Lu, and D. Akinwande, Fabrication, Characterization and Applications of Graphene Electronic Tattoos, Nat Protoc 16, 2395 (2021).

[76] B. Ji, Q. Zhou, B. Hu, J. Zhong, J. Zhou, and B. Zhou, Bio-Inspired Hybrid Dielectric for Capacitive and Triboelectric Tactile Sensors with High Sensitivity and Ultrawide Linearity Range, Advanced Materials 33, 2100859 (2021).

[77] P. Wang, G. Li, J. Liu, Z. Hou, C. Meng, S. Guo, C. Liu, and S. Fan, Tailorable Capacitive Tactile Sensor Based on Stretchable and Dissolvable Porous Silver Nanowire/Polyvinyl Alcohol Nanocomposite Hydrogel for Wearable Human Motion Detection, Advanced Materials Interfaces 8, 2100998 (2021).

[78] G. G. Wallace, T. E. Campbell, and P. C. Innis, Putting Function into Fashion: Organic Conducting Polymer Fibres and Textiles, Fibers Polym 8, 135 (2007).

[79] M. Liu, G. Lake-Thompson, A. Wescott, S. Beeby, J. Tudor, and K. Yang, Design and Development of a Stretchable Electronic Textile and Its Application in a Knee Sleeve Targeting Wearable Pain Management, Sensors and Actuators A: Physical 369, 115102 (2024).

[80] M. T. Hossain, M. A. Shahid, M. G. M. Limon, I. Hossain, and N. Mahmud, Techniques, Applications, and Challenges in Textiles for a Sustainable Future, Journal of Open Innovation: Technology, Market, and Complexity 10, 100230 (2024).

[81] K. Zhao, W. Niu, and S. Zhang, Highly Stretchable, Breathable and Negative Resistance Variation Textile Strain Sensor with Excellent Mechanical Stability for Wearable Electronics, J Mater Sci 55, 2439 (2020).

[82] K. Rajan, E. Garofalo, and A. Chiolerio, Wearable Intrinsically Soft, Stretchable, Flexible Devices for Memories and Computing, Sensors 18, 2 (2018).

[83] S. Dong, F. Xu, Y. Sheng, Z. Guo, X. Pu, and Y. Liu, Seamlessly Knitted Stretchable Comfortable Textile Triboelectric Nanogenerators for E-Textile Power Sources, Nano Energy 78, 105327 (2020).

[84] T.-G. La, S. Qiu, D. K. Scott, R. Bakhtiari, J. W. P. Kuziek, K. E. Mathewson, J. Rieger, and H.-J. Chung, Two-Layered and Stretchable e-Textile Patches for Wearable Healthcare Electronics, Advanced Healthcare Materials 7, 1801033 (2018).

[85] T. Vervust, G. Buyle, F. Bossuyt, and J. Vanfleteren, Integration of Stretchable and Washable Electronic Modules for Smart Textile Applications, The Journal of The Textile Institute 103, 1127 (2012).

[86] B. Tian et al., Fully Printed Stretchable and Multifunctional E-Textiles for Aesthetic Wearable Electronic Systems, Small 18, 2107298 (2022).

[87] M. Sala de Medeiros, D. Goswami, D. Chanci, C. Moreno, and R. V. Martinez, Washable, Breathable, and Stretchable e-Textiles Wirelessly Powered

by Omniphobic Silk-Based Coils, Nano Energy 87, 106155 (2021).

[88] L. Wang, X. Fu, J. He, X. Shi, T. Chen, P. Chen, B. Wang, and H. Peng, Application Challenges in Fiber and Textile Electronics, Advanced Materials 32, 1901971 (2020).

[89] T. Hughes-Riley, T. Dias, and C. Cork, A Historical Review of the Development of Electronic Textiles, Fibers 6, 2 (2018).

[90] J. S. Heo, J. Eom, Y.-H. Kim, and S. K. Park, Recent Progress of Textile-Based Wearable Electronics: A Comprehensive Review of Materials, Devices, and Applications, Small 14, 1703034 (2018).

[91] M. R. Miah, M. Yang, M. M. Hossain, S. Khandaker, and Md. R. Awual, Textile-Based Flexible and Printable Sensors for next Generation Uses and Their Contemporary Challenges: A Critical Review, Sensors and Actuators A: Physical 344, 113696 (2022).

[92] N. A. Choudhry, L. Arnold, A. Rasheed, I. A. Khan, and L. Wang, Textronics—A Review of Textile-Based Wearable Electronics, Advanced Engineering Materials 23, 2100469 (2021).

[93] C. Wang, T. Yokota, and T. Someya, Natural Biopolymer-Based Biocompatible Conductors for Stretchable Bioelectronics, Chem. Rev. 121, 2109 (2021).

[94] Y. Li, W. Cao, Z. Liu, Y. Zhang, Z. Chen, and X. Zheng, A Personalized Electronic Textile for Ultrasensitive Pressure Sensing Enabled by Biocompatible MXene/PEDOT:PSS Composite, Carbon Energy 6, e530 (2024).

[95] C. Zhi, S. Shi, S. Meng, H. Wu, Y. Si, K. Zhang, S. Zhang, and J. Hu, A Biocompatible and Antibacterial All-Textile Structured Triboelectric Nanogenerator for Self-Powered Tactile Sensing, Nano Energy 115, 108734 (2023).

[96] T. Xing et al., Silk-Based Flexible Electronics and Smart Wearable Textiles: Progress and Beyond, Chemical Engineering Journal 474, 145534 (2023).

[97] M. Irimia-Vladu, “Green” Electronics: Biodegradable and Biocompatible Materials and Devices for Sustainable Future, Chemical Society Reviews 43, 588 (2014).

[98] Z. Hui, L. Zhang, G. Ren, G. Sun, H.-D. Yu, and W. Huang, Green Flexible Electronics: Natural Materials, Fabrication, and Applications, Advanced Materials 35, 2211202 (2023).

[99] S. Ling, Z. Qin, C. Li, W. Huang, D. L. Kaplan, and M. J. Buehler, Polymorphic Regenerated Silk Fibers Assembled through Bioinspired Spinning, Nat Commun 8, 1387 (2017).

[100] D. Meoli and T. May-Plumlee, Interactive Electronic Textile Development: A Review of Technologies, Journal of Textile Apparel Technology Management 2, (2002).

[101] H. M. Lee, S.-Y. Choi, A. Jung, and S. H. Ko, Highly Conductive Aluminum Textile and Paper for Flexible and Wearable Electronics, Angewandte Chemie 125, 7872 (2013).

[102] H. M. Lee, H. B. Lee, D. S. Jung, J.-Y. Yun, S. H. Ko, and S. B. Park, Solution Processed Aluminum Paper for Flexible Electronics, Langmuir 28, 13127 (2012).

[103] E. Dokur, S. Uruc, R. Kurteli, O. Gorduk, and Y. Sahin, Investigation of Flexible Electrochemical Sensor Properties of Graphite Conductive Ink Modified Textile Products and Their Applications in Electrical Circuits, Materials Today Communications 37, 106920 (2023).

[104] B. Tian, K. Zheng, R. Yu, X. Chen, P. Guo, Y. Wu, J. Liang, and W. Wu, High Performance Fully-Printed Strain-Sensing e-Textile for Human Posture Recognition, Chemical Engineering Journal 475, 146197 (2023).

[105] X. Zeng, M. Hu, P. He, W. Zhao, S. Dong, X. Xu, G. Dai, J. Sun, and J. Yang, Highly Conductive Carbon-Based E-Textile for Gesture Recognition, IEEE

Electron Device Letters 44, 825 (2023).

[106] P. Zhang, CHAPTER 4 - Transducers and Valves, in Advanced Industrial Control Technology, edited by P. Zhang (William Andrew Publishing, Oxford, 2010), pp. 117–152.

[107] P. Regtien and E. Dertien, 1 - Introduction, in Sensors for Mechatronics (Second Edition), edited by P. Regtien and E. Dertien (Elsevier, 2018), pp. 1–22.

[108] Z. Wang, Y. Li, S. Wu, Y. Zhou, L. Yang, Y. Xu, T. Zhang, and Q. Pan, A Survey on Cybersecurity Attacks and Defenses for Unmanned Aerial Systems, Journal of Systems Architecture 138, 102870 (2023).

[109] C. Paladiya and A. Kiani, Nano Structured Sensing Surface: Significance in Sensor Fabrication, Sensors and Actuators B: Chemical 268, 494 (2018).

[110] R. Megha, F. A. Ali, Y. T. Ravikiran, C. H. V. V. Ramana, A. B. V. Kiran Kumar, D. K. Mishra, S. C. Vijayakumari, and D. Kim, Conducting Polymer Nanocomposite Based Temperature Sensors: A Review, Inorganic Chemistry Communications 98, 11 (2018).

[111] E. Borràs, J. Ferré, R. Boqué, M. Mestres, L. Aceña, and O. Busto, Data Fusion Methodologies for Food and Beverage Authentication and Quality Assessment – A Review, Analytica Chimica Acta 891, 1 (2015).

[112] P. Boyraz, G. Runge, and A. Raatz, An Overview of Novel Actuators for Soft Robotics, Actuators 7, 3 (2018).

[113] J. Kim, J. W. Kim, H. C. Kim, L. Zhai, H.-U. Ko, and R. M. Muthoka, Review of Soft Actuator Materials, Int. J. Precis. Eng. Manuf. 20, 2221 (2019).

[114] A. A. Basheer, Graphene Materials for Fabrication of Robots, Materials Chemistry and Physics 302, 127781 (2023).

[115] C. Cochrane and A. Cayla, 5 - Polymer-Based Resistive Sensors for Smart Textiles, in Multidisciplinary Know-How for Smart-Textiles Developers, edited by

T. Kirstein (Woodhead Publishing, 2013), pp. 129–153.

[116] S. Saga, Physical Sensors: Mechanical Sensors, in Encyclopedia of Sensors and Biosensors (First Edition), edited by R. Narayan (Elsevier, Oxford, 2023), pp. 62–75.

[117] J. X. J. Zhang and K. Hoshino, Chapter 6 - Mechanical Transducers: Cantilevers, Acoustic Wave Sensors, and Thermal Sensors, in Molecular Sensors and Nanodevices (Second Edition), edited by J. X. J. Zhang and K. Hoshino (Academic Press, 2019), pp. 311–412.

[118] Y. Yang, S. Ding, B. Plovie, W. Li, and C. Shang, Soft and Stretchable Electronics Design, in Encyclopedia of Sensors and Biosensors (First Edition), edited by R. Narayan (Elsevier, Oxford, 2023), pp. 258–286.

[119] Z. G. Wu, 16 - Microfluidic Devices Using Flexible Organic Electronic Materials, in Handbook of Flexible Organic Electronics, edited by S. Logothetidis (Woodhead Publishing, Oxford, 2015), pp. 397–412.

[120] L. Tang, S. Wu, J. Qu, L. Gong, and J. Tang, A Review of Conductive Hydrogel Used in Flexible Strain Sensor, Materials 13, 18 (2020).

[121] H. Chen, Y. Liu, B. Ren, Y. Zhang, J. Ma, L. Xu, Q. Chen, and J. Zheng, Super Bulk and Interfacial Toughness of Physically Crosslinked Double-Network Hydrogels, Advanced Functional Materials 27, 1703086 (2017).

[122] H.-J. Li, H. Jiang, and K. Haraguchi, Ultrastiff, Thermoresponsive Nanocomposite Hydrogels Composed of Ternary Polymer–Clay–Silica Networks, Macromolecules 51, 529 (2018).

[123] Z. Qin, R. Niu, C. Tang, J. Xia, F. Ji, D. Dong, H. Zhang, S. Zhang, J. Li, and F. Yao, A Dual-Crosslinked Strategy to Construct Physical Hydrogels with High Strength, Toughness, Good Mechanical Recoverability, and Shape-Memory Ability, Macromolecular Materials and Engineering 303, 1700396 (2018).

[124] M. Li, S. Chen, B. Fan, B. Wu, and X. Guo, Printed Flexible Strain Sensor Array for Bendable Interactive Surface, Advanced Functional Materials 30, 2003214 (2020).

[125] J. Wang, C. Lu, and K. Zhang, Textile-Based Strain Sensor for Human Motion Detection, ENERGY ENVIRONMENTAL MATERIALS 3, 80 (2020).

[126] J. Zhang, Y. Zhang, Y. Li, and P. Wang, Textile-Based Flexible Pressure Sensors: A Review, Polymer Reviews 62, 65 (2022).

[127] U. Pierre Claver and G. Zhao, Recent Progress in Flexible Pressure Sensors Based Electronic Skin, Advanced Engineering Materials 23, 2001187 (2021).

[128] H. Liu, H. Zhang, W. Han, H. Lin, R. Li, J. Zhu, and W. Huang, 3D Printed Flexible Strain Sensors: From Printing to Devices and Signals, Advanced Materials 33, 2004782 (2021).

[129] S. M. Ng, 12 - Carbon Dots as Optical Nanoprobes for Biosensors, in Nanobiosensors for Biomolecular Targeting, edited by S. C. B. Gopinath and T. Lakshmipriya (Elsevier, 2019), pp. 269–300.

[130] N. Sabri, S. A. Aljunid, M. S. Salim, R. B. Ahmad, and R. Kamaruddin, Toward Optical Sensors: Review and Applications, J. Phys.: Conf. Ser. 423, 012064 (2013).

[131] G. Manjavacas and B. Nieto, 10 - Hydrogen Sensors and Detectors, in Compendium of Hydrogen Energy, edited by M. Ball, A. Basile, and T. N. Veziroğlu (Woodhead Publishing, Oxford, 2016), pp. 215–234.

[132] G. Owojaiye and Y. Sun, Focal Design Issues Affecting the Deployment of Wireless Sensor Networks for Pipeline Monitoring, Ad Hoc Networks 11, 1237 (2013).

[133] E. Tapanes, FIBRE OPTIC SENSING SOLUTIONS FOR REAL-TIME PIPELINE INTEGRITY MONITORING, in (n.d.).

[134] J. R. Askim, M. Mahmoudi, and K. S. Suslick, Optical Sensor Arrays for Chemical Sensing: The Optoelectronic Nose, Chemical Society Reviews 42, 8649 (2013).

[135] C. Jiang, Z. Zhang, J. Pan, Y. Wang, L. Zhang, and L. Tong, Finger-Skin-Inspired Flexible Optical Sensor for Force Sensing and Slip Detection in Robotic Grasping, Advanced Materials Technologies 6, 2100285 (2021).

[136] Z.-L. Lei and B. Guo, 2D Material-Based Optical Biosensor: Status and Prospect, Advanced Science 9, 2102924 (2022).

[137] W. Chen, X. Ma, H. Chen, S. Hua Liu, and J. Yin, Fluorescent Probes for pH and Alkali Metal Ions, Coordination Chemistry Reviews 427, 213584 (2021).

[138] V. Kumar, S. K. Raghuwanshi, and S. Kumar, Recent Advances in Carbon Nanomaterials Based SPR Sensor for Biomolecules and Gas Detection—A Review, IEEE Sensors Journal 22, 15661 (2022).

[139] S. Das, R. Devireddy, and M. R. Gartia, Surface Plasmon Resonance (SPR) Sensor for Cancer Biomarker Detection, Biosensors 13, 3 (2023).

[140] T. Dinh, T. Nguyen, H.-P. Phan, V. Dau, D. Dao, and N.-T. Nguyen, Physical Sensors: Thermal Sensors, in Encyclopedia of Sensors and Biosensors (First Edition), edited by R. Narayan (Elsevier, Oxford, 2023), pp. 20–33.

[141] J. T. W. Kuo, L. Yu, and E. Meng, Micromachined Thermal Flow Sensors—A Review, Micromachines 3, 3 (2012).

[142] N. T. Nguyen, Micromachined Flow Sensors—a Review, Flow Measurement and Instrumentation 8, 7 (1997).

[143] L. A. Beardslee, A. M. Addous, S. Heinrich, F. Josse, I. Dufour, and O. Brand, Thermal Excitation and Piezoresistive Detection of Cantilever In-Plane Resonance Modes for Sensing Applications, Journal of Microelectromechanical Systems 19, 1015 (2010).

[144] Y. Su et al., Printable, Highly Sensitive Flexible Temperature Sensors for Human Body Temperature Monitoring: A Review, Nanoscale Res Lett 15, 200 (2020).

[145] E. Sowade, H. Kang, K. Y. Mitra, O. J. Weiß, J. Weber, and R. R. Baumann, Roll-to-Roll Infrared (IR) Drying and Sintering of an Inkjet-Printed Silver Nanoparticle Ink within 1 Second, Journal of Materials Chemistry C 3, 11815 (2015).

[146] H. Menon, R. Aiswarya, and K. Peethambharan Surendran, Screen Printable MWCNT Inks for Printed Electronics, RSC Advances 7, 44076 (2017).

[147] J. Wu, Z. Wu, Y. Wei, H. Ding, W. Huang, X. Gui, W. Shi, Y. Shen, K. Tao, and X. Xie, Ultrasensitive and Stretchable Temperature Sensors Based on Thermally Stable and Self-Healing Organohydrogels, ACS Appl. Mater. Interfaces 12, 19069 (2020).

[148] Y. H. Jung, S. K. Hong, H. S. Wang, J. H. Han, T. X. Pham, H. Park, J. Kim, S. Kang, C. D. Yoo, and K. J. Lee, Flexible Piezoelectric Acoustic Sensors and Machine Learning for Speech Processing, Advanced Materials 32, 1904020 (2020).

[149] M. J. Vellekoop, Acoustic Wave Sensors and Their Technology, Ultrasonics 36, 7 (1998).

[150] G. M. Sessler, Acoustic Sensors, Sensors and Actuators A: Physical 26, 323 (1991).

[151] Y. Bai, L. Lu, J. Cheng, J. Liu, Y. Chen, and J. Yu, Acoustic-Based Sensing and Applications: A Survey, Computer Networks 181, 107447 (2020).

[152] K. Takagi, Fundamentals of Ultrasonic Spectroscopy, Jpn. J. Appl. Phys. 25, 3 (1986).

[153] S. Lee, J. Kim, H. Roh, W. Kim, S. Chung, W. Moon, and K. Cho, A

High-Fidelity Skin-Attachable Acoustic Sensor for Realizing Auditory Electronic Skin, Advanced Materials 34, 2109545 (2022).

[154] J. Wu, C. Yin, J. Zhou, H. Li, Y. Liu, Y. Shen, S. Garner, Y. Fu, and H. Duan, Ultrathin Glass-Based Flexible, Transparent, and Ultrasensitive Surface Acoustic Wave Humidity Sensor with ZnO Nanowires and Graphene Quantum Dots, ACS Appl. Mater. Interfaces 12, 39817 (2020).

[155] Y. Huang, P. Kr. Das, and V. R. Bhethanabotla, Surface Acoustic Waves in Biosensing Applications, Sensors and Actuators Reports 3, 100041 (2021).

[156] S. Li and V. R. Bhethanabotla, Design of a Portable Orthogonal Surface Acoustic Wave Sensor System for Simultaneous Sensing and Removal of Non-specifically Bound Proteins, Sensors 19, 18 (2019).

[157] V. B. Kandimalla, V. S. Tripathi, and H. Ju, CHAPTER 16 - Biosensors Based on Immobilization of Biomolecules in Sol-Gel Matrices, in Electrochemical Sensors, Biosensors and Their Biomedical Applications, edited by X. Zhang, H. Ju, and J. Wang (Academic Press, San Diego, 2008), pp. 503–529.

[158] N. M. Kulshreshtha, D. Shrivastava, and P. S. Bisen, 14 - Contaminant Sensors: Nanotechnology-Based Contaminant Sensors, in Nanobiosensors, edited by A. M. Grumezescu (Academic Press, 2017), pp. 573–628.

[159] Y. Wang, K. Liu, M. Zhang, T. Xu, H. Du, B. Pang, and C. Si, Sustainable Polysaccharide-Based Materials for Intelligent Packaging, Carbohydrate Polymers 313, 120851 (2023).

[160] E. B. Bahadır and M. K. Sezgintürk, 8 - Biosensor Technologies for Analyses of Food Contaminants, in Nanobiosensors, edited by A. M. Grumezescu (Academic Press, 2017), pp. 289–337.

[161] A. M. Vaidya and U. S. Annapure, Chapter 38 - Enzymes in Biosensors for Food Quality Assessment, in Enzymes in Food Biotechnology, edited by M. Kuddus (Academic Press, 2019), pp. 659–674.

[162] S. Hameed, L. Xie, and Y. Ying, Conventional and Emerging Detection Techniques for Pathogenic Bacteria in Food Science: A Review, Trends in Food Science Technology 81, 61 (2018).

[163] K. A. Lamkin-Kennard and M. B. Popovic, 4 - Sensors: Natural and Synthetic Sensors, in Biomechatronics, edited by M. B. Popovic (Academic Press, 2019), pp. 81–107.

[164] N. S. Sworna, A. K. M. M. Islam, S. Shatabda, and S. Islam, Towards Development of IoT-ML Driven Healthcare Systems: A Survey, Journal of Network and Computer Applications 196, 103244 (2021).

[165] F. Mandoj, S. Nardis, C. Di Natale, and R. Paolesse, Porphyrinoid Thin Films for Chemical Sensing, in Encyclopedia of Interfacial Chemistry, edited by K. Wandelt (Elsevier, Oxford, 2018), pp. 422–443.

[166] F. Faridbod, M. R. Ganjali, and M. Hosseini, 12 - Lanthanide Materials as Chemosensors, in Lanthanide-Based Multifunctional Materials, edited by P. Martín-Ramos and M. Ramos Silva (Elsevier, 2018), pp. 411–454.

[167] S. Kumar, S. Tripathy, A. Jyoti, and S. G. Singh, Recent Advances in Biosensors for Diagnosis and Detection of Sepsis: A Comprehensive Review, Biosensors and Bioelectronics 124–125, 205 (2019).

[168] M. Miyake, Chapter 26 - Electrochemical Functions, in Carbon Alloys, edited by E. Yasuda, M. Inagaki, K. Kaneko, M. Endo, A. Oya, and Y. Tanabe (Elsevier Science, Oxford, 2003), pp. 435–445.

[169] R. Li et al., A Flexible and Physically Transient Electrochemical Sensor for Real-Time Wireless Nitric Oxide Monitoring, Nat Commun 11, 3207 (2020).

[170] C. Zhu, H. Xue, H. Zhao, T. Fei, S. Liu, Q. Chen, B. Gao, and T. Zhang, A Dual-Functional Polyaniline Film-Based Flexible Electrochemical Sensor for the Detection of pH and Lactate in Sweat of the Human Body, Talanta 242, 123289 (2022).

[171] K. Keshyagol, S. Hiremath, V. H. M., and P. Hiremath, Estimation of Energy Storage Capability of the Parallel Plate Capacitor Filled with Distinct Dielectric Materials, Engineering Proceedings 59, 1 (2023).

[172] A. S. Abu-Abed and R. G. Lindquist, CAPACITIVE INTERDIGITAL SENSOR WITH INHOMOGENEOUS NEMATIC LIQUID CRYSTAL FILM, PIER B 7, 75 (2008).

[173] A. S. Thakur, V. Srivatava, H. K. B. Park, I. Kebaili, I. Boukhris, Y. H. Joo, T. H. Sung, A. Kumar, and R. Vaish, Calligraphic Interdigitated Capacitive Sensors for Green Electronics, Sci Rep 14, 15685 (2024).

[174] P. M. Hall, Resistance Calculations for Thin Film Rectangles, Thin Solid Films 300, 256 (1997).

[175] S. Palanisamy, V. Tunakova, J. Ornstova, M. Vysanska, and J. Militky, The Effect of Tensile Deformation of Knitted Fabrics on Their Electromagnetic Shielding Ability, Electrical Resistance, and Porosity, Journal of Industrial Textiles 54, 15280837241239232 (2024).

[176] C. V. Raman and K. S. Krishnan, A New Type of Secondary Radiation, Nature 121, 501 (1928).

[177] G. S. Bumbrah and R. M. Sharma, Raman Spectroscopy – Basic Principle, Instrumentation and Selected Applications for the Characterization of Drugs of Abuse, Egyptian Journal of Forensic Sciences 6, 209 (2016).

[178] S. Sharma, S. Jaiswal, B. Duffy, and A. K. Jaiswal, Nanostructured Materials for Food Applications: Spectroscopy, Microscopy and Physical Properties, Bioengineering 6, 1 (2019).

[179] D. N. G. Krishna and J. Philip, Review on Surface-Characterization Applications of X-Ray Photoelectron Spectroscopy (XPS): Recent Developments and Challenges, Applied Surface Science Advances 12, 100332 (2022).

[180] J.-F. Lataste, 12 - Electrical Resistivity for the Evaluation of Reinforced Concrete Structures, in Non-Destructive Evaluation of Reinforced Concrete Structures, edited by C. Maierhofer, H.-W. Reinhardt, and G. Dobmann, Vol. 2 (Woodhead Publishing, 2010), pp. 243–275.

[181] M. Darmi, L. Cherif, J. Benallal, R. Elgouri, and N. Hmina, Integrated Circuit Conception: A Wire Optimization Technic Reducing Interconnection Delay in Advanced Technology Nodes, Electronics 6, 4 (2017).

[182] M. Simić, Realization of Digital LCR Meter, in 2014 International Conference and Exposition on Electrical and Power Engineering (EPE) (2014), pp. 769–773.

[183] G. L. Zeng and M. Zeng, Voltage Divider and Current Divider, in Electric Circuits: A Concise, Conceptual Tutorial, edited by G. L. Zeng and M. Zeng (Springer International Publishing, Cham, 2021), pp. 43–48.

[184] M. V. Sefton, H. Uludag, J. Babensee, T. Roberts, V. Horvath, and U. De Boni, 22 - Microencapsulation of Cells in Thermoplastic Copolymer (Hydroxyethyl Methacrylate–Methyl Methacrylate), in Methods in Neurosciences, edited by T. R. Flanagan, D. F. Emerich, and S. R. Winn, Vol. 21 (Academic Press, 1994), pp. 371–386.

[185] L. Gutiérrez, G. Stepien, L. Gutiérrez, M. Pérez-Hernández, J. Pardo, J. Pardo, V. Grazú, and J. M. de la Fuente, 1.09 - Nanotechnology in Drug Discovery and Development, in Comprehensive Medicinal Chemistry III, edited by S. Chackalamannil, D. Rotella, and S. E. Ward (Elsevier, Oxford, 2017), pp. 264–295.

[186] W. S. de Almeida and D. A. da Silva, Does Polysaccharide Quaternization Improve Biological Activity?, International Journal of Biological Macromolecules 182, 1419 (2021).

[187] S. Chen, Y. Jiang, M. Fan, X. Zhang, Y. Zhang, T. Chen, C. Yang, W.-C. Law, Z. Xu, and G. Xu, Highly Biocompatible Chlorin E6-Poly(Dopamine)

Core–Shell Nanoparticles for Enhanced Cancer Phototherapy, Nanoscale Advances 4, 4617 (2022).

[188] K. M. McKinnon, Flow Cytometry: An Overview, Current Protocols in Immunology 120, 5.1.1 (2018).

[189] N. Sharma, R. Dev Gupta, R. Chandmal Sharma, S. Dayal, and A. Singh Yadav, Graphene: An Overview of Its Characteristics and Applications, Materials Today: Proceedings 47, 2752 (2021).

[190] A. R. Urade, I. Lahiri, and K. S. Suresh, Graphene Properties, Synthesis and Applications: A Review, JOM 75, 614 (2023).

[191] W. Wu, H.-Y. Liu, Y. Kang, T. Zhang, S. Jiang, B. Li, J. Yin, and J. Zhu, Synergistic Combination of Carbon-Black and Graphene for 3D Printable Stretchable Conductors, Materials Technology 37, 1971 (2022).

[192] R.-Y. Zhang, M. Gao, W.-R. Liu, W.-H. Chiang, and L.-H. Yeh, A Graphene/Carbon Black Nanofluidic Membrane with Fast Ion Transport for Enhanced Electrokinetic Energy Generation, Carbon 204, 1 (2023).

[193] F. Shahamatifard, D. Rodrigue, K.-W. Park, S. Frikha, and F. Mighri, Synergistic Effect between Graphene Nanoplatelets and Carbon Black to Improve the Thermal and Mechanical Properties of Natural Rubber Nanocomposites, Polymer-Plastics Technology and Materials 61, 1578 (2022).

[194] S. Chandramohan, M. Vaithiyanathan, B. C. Chakraborty, and M. M. Dharmaraj, Synergistic Effect of Graphene and Carbon Black on the Mechanical and Vibration Damping Characteristics of Styrene-Butadiene Rubber, Iran Polym J (2024).

[195] L. Valentini, S. Bittolo Bon, M. A. Lopez-Manchado, R. Verdejo, L. Pappalardo, A. Bolognini, A. Alvino, S. Borsini, A. Berardo, and N. M. Pugno, Synergistic Effect of Graphene Nanoplatelets and Carbon Black in Multifunctional EPDM Nanocomposites, Composites Science and Technology 128, 123 (2016).

[196] Y. Zhang, L. Deng, H. Lv, and G. Chen, Toward Improved Trade-off between Thermoelectric and Mechanical Performances in Polycarbonate/Single-Walled Carbon Nanotube Composite Films, Npj Flex Electron 4, 1 (2020).

[197] S.-Y. Ku, C. D. Liman, J. E. Cochran, M. F. Toney, M. L. Chabinyc, and C. J. Hawker, Solution-Processed Nanostructured Benzoporphyrin with Polycarbonate Binder for Photovoltaics, Advanced Materials 23, 2289 (2011).

[198] T. M. Eggenhuisen and T. L. Hoeks, Degradation Mechanisms of Aromatic Polycarbonate, in Reliability of Organic Compounds in Microelectronics and Optoelectronics: From Physics-of-Failure to Physics-of-Degradation, edited by W. D. van Driel and M. Yazdan Mehr (Springer International Publishing, Cham, 2022), pp. 33–52.

[199] T. Artham and M. Doble, Biodegradation of Aliphatic and Aromatic Polycarbonates, Macromolecular Bioscience 8, 14 (2008).

[200] J. Hong, M. K. Park, E. J. Lee, D. Lee, D. S. Hwang, and S. Ryu, Origin of New Broad Raman D and G Peaks in Annealed Graphene, Sci Rep 3, 2700 (2013).

[201] E. Dervishi, Z. Ji, H. Htoon, M. Sykora, and S. K. Doorn, Raman Spectroscopy of Bottom-up Synthesized Graphene Quantum Dots: Size and Structure Dependence, Nanoscale 11, 16571 (2019).

[202] L. M. Malard, M. A. Pimenta, G. Dresselhaus, and M. S. Dresselhaus, Raman Spectroscopy in Graphene, Physics Reports 473, 51 (2009).

[203] A. C. Ferrari, Raman Spectroscopy of Graphene and Graphite: Disorder, Electron–Phonon Coupling, Doping and Nonadiabatic Effects, Solid State Communications 143, 47 (2007).

[204] M. Youssry, F. Z. Kamand, M. I. Magzoub, and M. S. Nasser, Aqueous Dispersions of Carbon Black and Its Hybrid with Carbon Nanofibers, RSC Adv. 8, 32119 (2018).

[205] A. Kirakosyan, D. Lee, Y. Choi, N. Jung, and J. Choi, Poly(Styrene Sulfonic Acid)-Grafted Carbon Black Synthesized by Surface-Initiated Atom Transfer Radical Polymerization, Molecules 28, 10 (2023).

[206] G. Gao, D. Liu, S. Tang, C. Huang, M. He, Y. Guo, X. Sun, and B. Gao, Heat-Initiated Chemical Functionalization of Graphene, Sci Rep 6, 20034 (2016).

[207] D. Ristiani, R. Asih, F. Astuti, M. A. Baqiya, C. Kaewhan, S. Tunmee, H. Nakajima, S. Soontaranon, and Darminto, Mesostructural Study on Graphenic-Based Carbon Prepared from Coconut Shells by Heat Treatment and Liquid Exfoliation, Heliyon 8, e09032 (2022).

[208] P. M. Schlosser, A. S. Bale, C. F. Gibbons, A. Wilkins, and G. S. Cooper, Human Health Effects of Dichloromethane: Key Findings and Scientific Issues, Environmental Health Perspectives 123, 114 (2015).

[209] J. López-García, M. Lehocký, P. Humpolíček, and P. Sáha, HaCaT Keratinocytes Response on Antimicrobial Atelocollagen Substrates: Extent of Cytotoxicity, Cell Viability and Proliferation, Journal of Functional Biomaterials 5, 2 (2014).

[210] D. Bajpai and V. K. Tyagi, Laundry Detergents: An Overview, J Oleo Sci 56, 327 (2007).

[211] C. Mac Namara, A. Gabriele, C. Amador, and S. Bakalis, Dynamics of Textile Motion in a Front-Loading Domestic Washing Machine, Chemical Engineering Science 75, 14 (2012).

Appendix A

Code

A.1 Arduino Code for Strain Sensor Measurement

```
const int analogInPin = A0; // Analog input pin that the potentiometer is attached to

  int sensorValue = 0; // value read from the pot

  int outputValue = 0; // value output to the PWM (analog out)

  void setup()

  // initialize serial communications at 9600 bps:

  Serial.begin(1200);

  void loop()

  // read the analog in value:
```

```
sensorValue = analogRead(analogInPin);
// map it to the range of the analog out:
// outputValue = map(sensorValue, 0, 1023, 0, 5);
// change the analog out value:
Serial.println(sensorValue);
// wait 2 milliseconds before the next loop for the analog-to-digital
// converter to settle after the last reading:
delay(100);
```

Appendix B

Copyright Permission

Reference Number	License Supplier	License Number
[9]	Frontiers Media	Permission not required
[41]	Springer Nature	Permission not required
[42]	MDPI	Permission not required
[43]	Wiley	5853680271844
[44]	Elsevier	5853671048961
[175]	Sage Publishing	55853671278211

Table B.1: Declaration of Copyright Clearance Agreements